A WAVENUMBER INDEPENDENT BOUNDARY ELEMENT METHOD FOR AN ACOUSTIC SCATTERING PROBLEM*

S LANGDON[†‡] AND S N CHANDLER-WILDE[†§]

Abstract. In this paper we consider the impedance boundary value problem for the Helmholtz equation in a half-plane with piecewise constant boundary data, a problem which models, for example, outdoor sound propagation over inhomogeneous flat terrain. To achieve good approximation at high frequencies with a relatively low number of degrees of freedom we propose a novel Galerkin boundary element method, using a graded mesh with smaller elements adjacent to discontinuities in impedance and a special set of basis functions so that, on each element, the approximation space contains polynomials (of degree ν) multiplied by traces of plane waves on the boundary. We prove stability and convergence, and show that the error in computing the total acoustic field is $\mathcal{O}(N^{-(\nu+1)}\log^{1/2}N)$, where the number of degrees of freedom is proportional to $N\log N$. This error estimate is independent of the wavenumber, and thus the number of degrees of freedom required to achieve a prescribed level of accuracy does not increase as the wavenumber tends to infinity.

Key words. Galerkin method, high frequency, Helmholtz equation

AMS subject classifications. 35J05, 65R20

1. Introduction. High frequency scattering problems are of enormous interest to the mathematics, physics and engineering communities, with applications to electromagnetic scattering, radar problems, high frequency acoustics and geophysical waves. Although these problems have a long pedigree, their numerical solution continues to pose considerable difficulties. Many problems of scattering of time-harmonic acoustic or electromagnetic waves can be formulated as the Helmholtz equation

$$\Delta u + k^2 u = 0, \tag{1.1}$$

in $\mathbb{R}^d\backslash\Omega$, $d = 2, 3$, supplemented with appropriate boundary conditions. Here Ω is the scattering object and $k > 0$ (the wavenumber) is an arbitrary positive constant, proportional to the frequency of the incident wave.

Standard schemes for solving (1.1) become prohibitively expensive as $k \to \infty$. For standard boundary element or finite element schemes, where the approximation space typically consists of piecewise polynomials, the number of degrees of freedom per wavelength must remain fixed in order to maintain accuracy,with the rule of thumb in the engineering literature being a requirement for ten elements per wavelength. Often in applications this can result in excessively large systems when the wavelength is small compared to the size of the obstacle. These difficulties have been well documented, see for example [28, 29, 31]. For the finite element method the situation is arguably worse in that additional pollution effects are known to be important [5], these being phase errors in wave propagation across the domain, so that the degrees of freedom per wavelength need to increase somewhat to retain accuracy as k increases.

The development of more efficient numerical schemes for high frequency scattering problems has attracted much recent attention in the literature. In the case of boundary element methods, a great deal of effort has focused on the fast solution of the large systems which arise, using preconditioned iterative methods (e.g. [14]) combined with fast multipole (e.g. [16, 17]) or fast Fourier transform based methods (e.g.

*This work was supported by the EPSRC via grant GR/M59433/01

[†]Department of Mathematical Sciences, Brunel University, Uxbridge UB8 3PH, UK

[‡]*Email address:* masrswl@brunel.ac.uk

[§]*Email address:* mastsnc@brunel.ac.uk

[7]) to carry out the matrix-vector multiplications efficiently. The reduction in the computing cost achieved by the use of these schemes increases the upper limit on the frequency for which accurate results can be obtained in a reasonable time. However, as the size of the system still grows at least linearly with respect to k this upper limit is not removed altogether.

An increasingly popular approach in the literature for higher frequencies is to use either a finite element or a boundary element method in which the approximation space is enriched with plane wave or Bessel function solutions of (1.1), in order to represent efficiently the highly oscillatory solution when k is large. This idea has been applied to both finite element [26, 20] and boundary element schemes [28, 29], and other related methods include the microlocal discretisation approach [18, 16, 1], the ultra weak variational formulation [8] and the partition of unity method [25]. Promising numerical results have been reported for all these methods, but most are lacking in mathematical analysis, specifically with regard to how the error estimates depend on the wavenumber k.

The first method for which the dependence of the error estimates on the wavenumber k was specified is a microlocal discretisation approach for plane wave scattering by smooth convex obstacles in which a standard Galerkin boundary element method is applied to the ratio of the scattered field to the incident field [1]. The error estimate in this case is that the relative error in the best approximation from a boundary element space of piecewise polynomials of degree $\leq \nu$ is $\mathcal{O}(h^\nu) + \mathcal{O}((hk^{1/3})^{\nu+1})$. This result is clearly better than the (at least) linear dependence discussed previously. However the number of degrees of freedom needed to maintain accuracy is still predicted to grow like $k^{1/3}$ as k increases, and moreover the analysis does not guarantee that the Galerkin method solution is close to this best approximation in the limit as $k \to \infty$.

More recently, in [12], the authors and Ritter proposed a new high frequency boundary element method for a problem of acoustic scattering in 2-D by an inhomogeneous impedance plane, for which it was shown that the number of degrees of freedom needed to maintain accuracy as $k \to \infty$ grows only logarithmically with k. This appears to be the best theoretical estimate to date for any scattering problem in terms of the dependence on the wavenumber. In this paper we will be concerned with the numerical solution of the same problem, proposing modifications of the numerical scheme of [12]. For our modified scheme we are able to show, employing somewhat more elaborate arguments than those of [12], that for a fixed number of degrees of freedom the error is bounded independently of the wavenumber k. To our knowledge, this is the first such result for any scattering problem.

The problem we will consider is one of acoustic scattering of an incident wave by a planar surface with spatially varying acoustical surface impedance. This problem has attracted much attention in the literature (see for example [9, 10, 11, 13, 19, 21]), both in its own right and also as a model of the scattering of an incident acoustic or electromagnetic wave by an infinite rough surface [6, 30]. In the case in which there is no variation in the acoustical properties of the surface or the incident field in some fixed direction parallel to the surface, the problem is effectively two-dimensional. Adopting Cartesian coordinates $0x_1x_2x_3$, let this direction be that of the x_3-axis and the surface be the plane $x_2 = 0$. Assuming further that the incident wave and scattered fields are time harmonic, the total acoustic field $u^t \in \mathcal{C}(\overline{U}) \cap \mathcal{C}^2(U)$ then satisfies (1.1) in $U := \{(x_1, x_2) \in \mathbb{R}^2 : x_2 > 0\}$, supplemented with the impedance boundary condition

$$\frac{\partial u^t}{\partial x_2} + \mathrm{i}k\beta u^t = f, \quad \text{on } \Gamma := \{(x_1, 0) : x_1 \in \mathbb{R}\}, \tag{1.2}$$

with $f \equiv 0$, where $k = \omega/c > 0$. Here $\omega = 2\pi\mu$, μ is the frequency of the incident wave and c is the speed of sound in U. The acoustic pressure at time t, position (x_1, x_2, x_3) is then given by $\mathrm{Re}(\mathrm{e}^{-\mathrm{i}\omega t}u^t(x))$, for $x = (x_1, x_2) \in \overline{U}$.

In outdoor sound propagation, the relative surface admittance β depends on the frequency and the ground properties, and is often assumed in modelling to be piecewise constant, and constant outside some finite interval $[a, b]$ (see for example [10, 20, 22]), with β taking a different value for each ground surface type (grassland, forest floor, road pavement, etc. [4]). Thus, for some real numbers $a = t_0 < t_1 < \ldots < t_n = b$, the relative surface admittance at $(x_1, 0)$ on Γ is given by

$$\beta(x_1) = \begin{cases} \beta_j, & x_1 \in (t_{j-1}, t_j], \\ \beta_c, & x_1 \in \mathbb{R}\backslash(t_0, t_n]. \end{cases} \tag{1.3}$$

If the ground surface is to absorb rather than emit energy, the condition $\mathrm{Re}\beta \geq 0$ must be satisfied. We assume throughout that, for some $\epsilon > 0$,

$$\mathrm{Re}\beta_c \geq \epsilon, \quad \mathrm{Re}\beta_j \geq \epsilon, \quad |\beta_c| \leq \epsilon^{-1}, \quad |\beta_j| \leq \epsilon^{-1}, \quad j = 1, \ldots, n. \tag{1.4}$$

For simplicity of exposition, we restrict our attention to the case of plane wave incidence, so that the incident field u^i is given by $u^i(x) = \exp[\mathrm{i}k(x_1 \sin\theta - x_2 \cos\theta)]$, where $\theta \in (-\pi/2, \pi/2)$ is the angle of incidence. The reflected or scattered part of the wave field is $u := u^t - u^i \in C(\overline{U}) \cap C^2(U)$, and this also satisfies (1.1) and (1.2) with

$$f(x_1) := \mathrm{i}k\mathrm{e}^{\mathrm{i}kx_1 \sin\theta}(\cos\theta - \beta(x_1)), \quad x_1 \in \mathbb{R}. \tag{1.5}$$

In figure 1.1 we show scattering by a typical impedance plane. In this particular example, the surface admittance β is given by

$$\beta(x_1) = \begin{cases} 0.505 - 0.3\mathrm{i}, & x_1 \in (-5\lambda, 5\lambda], \\ 1, & x_1 \in \mathbb{R}\backslash(-5\lambda, 5\lambda], \end{cases}$$

where $\lambda = c/\mu = 2\pi/k$ is the wavelength. There are discontinuities in impedance at $x_1 = -5\lambda$ and at $x_1 = 5\lambda$. The incident plane wave ($\theta = \pi/4$ in this example) can be seen in the top left and the scattered wave in the top right of figure 1.1. This scattered wave is a combination of reflected and diffracted rays. The diffracted rays, propagating radially from the points $(-5\lambda, 0)$ and $(5\lambda, 0)$, can be seen more clearly in the bottom right of figure 1.1, where we have subtracted from the total field u^t the (known) total field in the case that $\beta \equiv 1$.

To achieve good approximations with a relatively low number of degrees of freedom, a boundary element method approach was used in [12] with ideas in the spirit of the geometrical theory of diffraction (GTD) being used to identify and subtract off the leading order behaviour (namely the incident and reflected rays) as $k \to \infty$. The remaining scattered wave (consisting of the rays diffracted at impedance discontinuities as visible in the lower right corner of figure 1.1) can then be expressed (on the boundary Γ) as the product of the known oscillatory functions $\mathrm{e}^{\pm\mathrm{i}kx_1}$ and unknown non-oscillatory functions denoted as $f_j^{\pm}$. Rigorous bounds were established in [12] on the derivatives of the non-oscillatory functions $f_j^{\pm}$ both adjacent to and away from discontinuities in impedance. Using these bounds a Galerkin method was developed, using a graded mesh with elements very large compared to the wavelength away from discontinuities in β, in order to take advantage of the smooth behaviour of $f_j^{\pm}$ away from these points, and a special set of basis functions so that on each element the

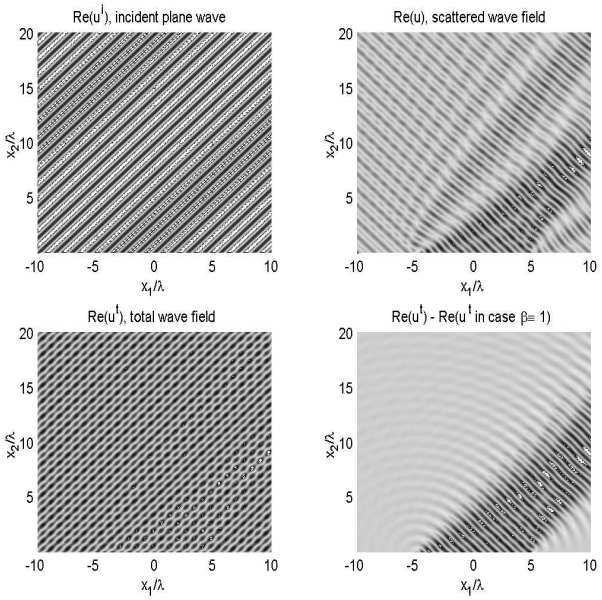

FIG. 1.1. *Acoustic scattering by an impedance boundary.*

approximation space consists of polynomials (of degree ν) multiplied by $\mathrm{e}^{\pm \mathrm{i}kx_1}$, so as to obtain a piecewise polynomial representation of the non-oscillatory functions $f_j^{\pm}$. Using this approach, it was shown in [12] that the error in computing an approximation to $u^t|_\Gamma$ on $[a,b]$ in the L_2 norm is $\mathcal{O}(\log^{\nu+3/2}(k(b-a))M^{-(\nu+1)})$ where M is the number of degrees of freedom.

In this paper we consider the same problem as in [12], and use a similar approach. We again subtract off the leading order behaviour as $k \to \infty$ on each interval, and again we express the scattered wave as a product of oscillatory and non-oscillatory functions. However, here (in §2) we prove sharper bounds on the non-oscillatory functions $f_j^{\pm}$ away from impedance discontinuities. Using these stronger bounds, in §3 we propose a similar Galerkin method to that in [12], but with a different approximation space. As in [12] this consists of polynomials (of degree ν) multiplied by $\mathrm{e}^{\pm \mathrm{i}kx_1}$, but unlike in [12] here the choice of whether to use $\mathrm{e}^{+\mathrm{i}kx_1}$ or $\mathrm{e}^{-\mathrm{i}kx_1}$ on each element is dictated by how close the relevant element is to each impedance discontinuity, and the graded mesh is chosen in a different way so that when k is large compared to N we do not discretise the entire domain. This is the key to achieving a convergence rate independent of the wavenumber.

In §3 we present an error analysis for this new approach, and we show that the error in computing an approximation to $u^t|_\Gamma$ on $[a,b]$ is $\mathcal{O}(N^{-(\nu+1)}\log^{1/2}|\min(N,k(b-a))|)$, in the L_2 norm, where the number of degrees of freedom is proportional to $N\log|\min(N,k(b-a))|$. As $\min(N,k(b-a)) \le N$, this error estimate shows that the error is bounded independently of k for a fixed number of degrees of freedom. We believe this to be the first result for any scattering problem where for a fixed discretisation the error does not grow at all as the size (in terms of number of wavelengths) of the scattering object to be discretised tends to infinity. Moreover, for fixed k, as $N \to \infty$, the extra logarithmic dependence on N of the error estimate and the number of degrees of freedom disappears, and we retain the same asymptotic convergence rate

as in [12].

Whereas in [12], results were only proved regarding the approximation of $u^t|_\Gamma$, here we also show, in theorem 3.6, that the total acoustic field at any point $x \in U$ can be computed to a similar order of accuracy. Finally in §4 we discuss the practical implementation of our approach, and we present some numerical results demonstrating that the theoretically predicted behaviour is achieved.

2. Integral equation formulation and regularity of the solution. In the rest of this paper, ν is the degree of the polynomial approximations used in the Galerkin method described in §3 below, and ϵ, in the range $0 < \epsilon < 1$, is the constant in the bound (1.4). Throughout C denotes an absolute constant, and C_ϵ, C_ν and $C_{\epsilon,\nu}$ denote constants depending only on ϵ, ν, and both ϵ and ν, respectively. Each is not necessarily the same at each occurence.

We begin by stating the problem we wish to solve precisely and reformulating it as an integral equation. For $H \geq 0$, let $U_H := \{(x_1, x_2) : x_2 > H\}$ and $\Gamma_H := \{(x_1, H) : x_1 \in \mathbb{R}\}$. To determine the scattered field u uniquely we impose the radiation condition proposed in [9] that, for some $H > 0$, u can be written in the half plane U_H as the double layer potential

$$u(x) = \int_{\Gamma_H} \frac{\partial H_0^{(1)}(k|x-y|)}{\partial y_2} \phi(y)\, \mathrm{d}s(y), \quad x \in U_H, \tag{2.1}$$

for some density $\phi \in L_\infty(\Gamma_H)$, where $H_0^{(1)}$ is the Hankel function of the first kind of order zero. The boundary value problem that we wish to solve for u is thus as follows:

Boundary Value Problem. *Given $k > 0$ (the wavenumber), $\theta \in (-\pi/2, \pi/2)$ (the angle of incidence) and β given by (1.3), find $u \in \mathcal{C}(\overline{U}) \cap \mathcal{C}^2(U)$ such that:*

(i) u is bounded in the horizontal strip $U \backslash U_H$ for every $H > 0$;

(ii) u satisfies the Helmholtz equation (1.1) in U;

(iii) u satisfies the impedance boundary condition (1.2) on Γ (in the weak sense explained in [9]), with $f \in L_\infty(\Gamma)$ given by (1.5);

(iv) u satisfies the radiation condition (2.1), for some $H > 0$ and $\phi \in L_\infty(\Gamma_H)$.

For $\beta^* \in \mathbb{C}$ with $\mathrm{Re}\beta^* > 0$ let $G_{\beta^*}(x, y)$ denote the Green's function for the above problem in the case of constant relative surface impedance, which satisfies (1.2), with $\beta \equiv \beta^*$ and $f \equiv 0$, and the standard Sommerfeld radiation and boundedness conditions. Explicit representations and efficient calculation methods for G_{β^*} are discussed in [11]. We shall require later the following bounds on G_{β^*} [12, (2.9),(2.10)], which hold provided $\mathrm{Re}\beta^* \geq \epsilon$ and $|\beta^*| \leq \epsilon^{-1}$:

$$|G_{\beta^*}(x, y)| \leq \frac{C_\epsilon(1 + kx_2)}{(k|x-y|)^{3/2}}, \quad x \in \overline{U},\ y \in \Gamma,\ x \neq y, \tag{2.2}$$

$$|G_{\beta^*}(x, y)| \leq C_\epsilon(1 - \log(k|x-y|)), \quad x \in \overline{U},\ y \in \Gamma,\ 0 < k|x-y| \leq 1. \tag{2.3}$$

The following result is shown in [12]:

THEOREM 2.1. *If u satisfies the above boundary value problem then*

$$u(x) = \int_\Gamma G_{\beta^*}(x, y)(\mathrm{i}k(\beta(y) - \beta^*)u(y) - f(y))\, \mathrm{d}s(y), \quad x \in \overline{U}. \tag{2.4}$$

Conversely, if $u|_\Gamma \in BC(\Gamma)$ (the space of bounded and continuous functions on Γ) and u satisfies (2.4), for some β^* with $\mathrm{Re}\beta^* > 0$, then u satisfies the above boundary

value problem. Moreover, equation (2.4) has exactly one solution with $u|_\Gamma \in BC(\Gamma)$*, and hence the boundary value problem has exactly one solution.*

We denote the (known) solution of the above boundary value problem in the special case $\beta \equiv \beta^*$ by u_{β^*}, and the corresponding total field by $u^t_{\beta^*} := u^i + u_{\beta^*}$. Then it is easily seen [12] that u_{β^*} is the plane wave $u_{\beta^*}(x) = R_{\beta^*}(\theta)\exp[\mathrm{i}k(x_1\sin\theta + x_2\cos\theta)]$, where $R_{\beta^*}(\theta) := (\cos\theta - \beta^*)/(\cos\theta + \beta^*)$ is a reflection coefficient. Moreover, it is shown rigorously in [12] that u^t satisfies

$$u^t(x) = u^t_{\beta^*}(x) + \mathrm{i}k\int_\Gamma G_{\beta^*}(x,y)(\beta(y) - \beta^*)u^t(y)\,\mathrm{d}s(y), \quad x \in \overline{U}. \tag{2.5}$$

We note that the approximate and numerical solution of this integral equation has been extensively studied, see for example [27, 21, 10, 19, 13, 12].

To make explicit the dependence on the wavenumber k in the results we obtain it is useful to introduce new, dimensionless variables. Thus, define $\phi(s) := u^t((s/k,0))$, $\psi_{\beta^*}(s) := u^t_{\beta^*}((s/k,0))$, and $\kappa_{\beta^*}(s) := G_{\beta^*}((s/k,0),(0,0))$, $s \in \mathbb{R}$. Then (2.5) restricted to Γ is the following second kind boundary integral equation for ϕ:

$$\phi(s) = \psi_{\beta^*}(s) + \mathrm{i}\int_{-\infty}^{\infty}\kappa_{\beta^*}(s-t)(\beta(t/k) - \beta^*)\phi(t)\,\mathrm{d}t, \quad s \in \mathbb{R}. \tag{2.6}$$

It is the main concern in the remainder of the paper to solve this equation numerically in the case when $\beta^* = \beta_c$. Clearly,

$$\psi_{\beta^*}(s) = (1 + R_{\beta^*}(\theta))\mathrm{e}^{\mathrm{i}s\sin\theta}, \tag{2.7}$$

and it is shown in [12], using the representation for G_{β^*} in [11], that

$$\kappa_{\beta^*}(s) = \frac{\mathrm{i}}{2}H_0^{(1)}(|s|) + \frac{\beta^{*2}\mathrm{e}^{\mathrm{i}|s|}}{\pi}\int_0^\infty \frac{t^{-1/2}e^{-|s|t}}{(t-2\mathrm{i})^{1/2}(t^2 - 2\mathrm{i}t - \beta^{*2})}\,\mathrm{d}t + C_{\beta^*}e^{\mathrm{i}|s|(1-\hat{a}_+)} \tag{2.8}$$

$$= \mathrm{e}^{\mathrm{i}|s|}\check{\kappa}_{\beta^*}(s), \quad s \in \mathbb{R}\backslash\{0\}, \tag{2.9}$$

where $\hat{a}_\pm := 1 \mp (1-\beta^{*2})^{\frac{1}{2}}$, with $\mathrm{Re}\{(1-\beta^{*2})^{1/2}\} \geq 0$,

$$C_{\beta^*} := \begin{cases} \frac{\beta^*}{(1-\beta^{*2})^{1/2}}, & \mathrm{Im}\beta^* < 0, \mathrm{Re}(\hat{a}_+) < 0, \\ \frac{\beta^*}{2(1-\beta^{*2})^{1/2}}, & \mathrm{Im}\beta^* < 0, \mathrm{Re}(\hat{a}_+) = 0, \\ 0, & \text{otherwise}, \end{cases}$$

and

$$\check{\kappa}_{\beta^*}(s) := \frac{1}{\pi}\int_0^\infty \frac{r^{\frac{1}{2}}(r-2\mathrm{i})^{\frac{1}{2}}}{r^2 - 2\mathrm{i}r - \beta^{*2}}\mathrm{e}^{-r|s|}\,\mathrm{d}r + C_{\beta^*}e^{-\mathrm{i}|s|\hat{a}_+}, \quad s \in \mathbb{R}\backslash\{0\}. \tag{2.10}$$

Clearly the only dependence on k in the known terms in (2.6) is in the impedance function $\beta(t/k)$. We shall see shortly that the oscillating part of $\kappa_{\beta^*}(s)$ is contained in the factor $\mathrm{e}^{\mathrm{i}|s|}$ in (2.9), $\check{\kappa}_{\beta^*}(s)$ becoming increasingly smooth as $s \to \pm\infty$.

In view of (1.3), if we set $\beta^* = \beta_c$ in (2.6), the interval of integration reduces to the finite interval $[\tilde{a}, \tilde{b}]$, where $\tilde{a} := ka = kt_0$, $\tilde{b} := kb = kt_n$. Explicitly, (2.6) becomes

$$\phi(s) = \psi_{\beta_c}(s) + \mathrm{i}\int_{\tilde{a}}^{\tilde{b}}\kappa_{\beta_c}(s-t)(\beta(t/k) - \beta_c)\phi(t)\,\mathrm{d}t, \quad s \in \mathbb{R}, \tag{2.11}$$

with ψ_{β_c} and κ_{β_c} given by (2.7) and (2.8) respectively with $\beta^* = \beta_c$. This integral equation is studied, in the case $\beta_c = 1$, in [9]. From [9, theorem 4.17] it follows that

$$\|\phi\|_\infty \le C_\epsilon \|\psi_1\|_\infty = C_\epsilon |1 + R_1(\theta)| \le C_\epsilon \cos\theta. \tag{2.12}$$

As in [12], and as discussed in the introduction, our numerical scheme for solving (2.11) is based on a consideration of the contribution of the reflected and diffracted ray paths in the spirit of the GTD. In particular, to leading order as $k \to \infty$, on the interval (t_{j-1}, t_j) it seems reasonable to suppose that the total field $\phi \approx \psi_{\beta_j}$, the total field there would be if the whole boundary had the admittance β_j of the interval (t_{j-1}, t_j), given explicitly by (2.7) with $\beta^* = \beta_j$. In fact, for $s \ne \tilde{t}_j := kt_j$, $j = 0, \dots, n$, it follows from theorem 2.3 below that $\phi(s) \to \Psi(s)$ as $k \to \infty$, where

$$\Psi(s) := \begin{cases} \psi_{\beta_j}(s), & s \in (\tilde{t}_{j-1}, \tilde{t}_j], \quad j = 1, \dots, n, \\ \psi_{\beta_c}(s), & s \in \mathbb{R} \backslash (\tilde{t}_0, \tilde{t}_n]. \end{cases} \tag{2.13}$$

In our numerical scheme we compute the difference between ϕ and Ψ, i.e.

$$\Phi(s) := \phi(s) - \Psi(s), \quad s \in \mathbb{R}, \tag{2.14}$$

which may be thought of as the correction to the leading order field due to scattering from impedance discontinuities. Clearly, from (2.11) we have that

$$\Phi = \Psi_\beta^{\beta_c} + K_\beta^{\beta_c} \Phi, \tag{2.15}$$

where $\Psi_\beta^{\beta_c} \in L_\infty(\mathbb{R})$ is given by $\Psi_\beta^{\beta_c} := \psi_{\beta_c} - \Psi + K_\beta^{\beta_c} \Psi$, and

$$K_\beta^{\beta_c} \chi(s) := \mathrm{i} \int_{\tilde{a}}^{\tilde{b}} \kappa_{\beta_c}(s-t)(\beta(t/k) - \beta_c)\chi(t)\,\mathrm{d}t.$$

Equation (2.15) will be the integral equation that we solve numerically. By setting $\beta^* = \beta_j$ in (2.6) we obtain explicit expressions for Φ on each subinterval, namely

$$\Phi(s) = \mathrm{e}^{\mathrm{i}s} f_j^+(s - \tilde{t}_{j-1}) + \mathrm{e}^{-\mathrm{i}s} f_j^-(\tilde{t}_j - s), \quad s \in (\tilde{t}_{j-1}, \tilde{t}_j],\ j = 1, \dots, n, \tag{2.16}$$

where for $j = 1, \dots, n$, $f_j^+, f_j^- \in \mathcal{C}[0, \infty)$ are defined by

$$f_j^+(r) := \int_{-\infty}^{\tilde{t}_{j-1}} \check{\kappa}_{\beta_j}(r + \tilde{t}_{j-1} - t)\mathrm{e}^{-\mathrm{i}t}\mathrm{i}(\beta(t/k) - \beta_j)\phi(t)\,\mathrm{d}t, \tag{2.17}$$

$$f_j^-(r) := \int_{\tilde{t}_j}^{\infty} \check{\kappa}_{\beta_j}(t - \tilde{t}_j + r)\mathrm{e}^{\mathrm{i}t}\mathrm{i}(\beta(t/k) - \beta_j)\phi(t)\,\mathrm{d}t, \tag{2.18}$$

with $\check{\kappa}_{\beta_j}$ given by (2.10) with $\beta^* = \beta_j$. Similarly, from (2.11),

$$\Phi(s) = \begin{cases} \mathrm{e}^{\mathrm{i}s} f_{n+1}^+(s - \tilde{t}_n), & s > \tilde{t}_n, \\ \mathrm{e}^{-\mathrm{i}s} f_0^-(\tilde{t}_0 - s), & s < \tilde{t}_0, \end{cases} \tag{2.19}$$

where f_{n+1}^+, f_0^- are given by (2.17), (2.18) respectively, with $\beta_0 := \beta_c$ and $\beta_{n+1} := \beta_c$.

The first term in (2.16) can be viewed as an explicit summation of all the diffracted rays scattered at the discontinuity in impedance at t_{j-1} which travel from left to right along (t_{j-1}, t_j). Similarly, the other term in (2.16) is the contribution to the

diffracted field diffracted by the discontinuity at t_j. In the remainder of this section, so as to design an efficient discretisation for Φ, we investigate in detail the behaviour of the integrals $f_j^{\pm}$. As a first step, we prove the following bounds on $|\check{\kappa}_{\beta^*}^{(m)}(s)|$, for $m = 0, 1, \ldots$, $s \in (0, \infty)$, which were stated without proof in [12].

LEMMA 2.2. *Suppose that* $\mathrm{Re}\beta^* \geq \epsilon$, $|\beta^*| \leq \epsilon^{-1}$ *hold for some* $\epsilon > 0$. *Then, for* $m = 0, 1, \ldots$, *there exist constants* c_m, *dependent only on* m *and* ϵ, *such that,*

$$|\check{\kappa}_{\beta^*}^{(m)}(s)| \leq \begin{cases} c_m(1 + |\log s|), & m = 0, \\ c_m s^{-m}, & m \geq 1, \end{cases} \quad \text{for } 0 \leq s \leq 1,$$
$$|\check{\kappa}_{\beta^*}^{(m)}(s)| \leq c_m s^{-\frac{3}{2}-m}, \quad \text{for } s > 1.$$

Proof. First, we define

$$F(z) := \frac{z^{1/2}(z-2\mathrm{i})^{1/2}}{z^2 - 2\mathrm{i}z - \beta^{*2}} = \frac{z^{1/2}(z-2\mathrm{i})^{1/2}}{(z-\mathrm{i}\hat{a}_+)(z-\mathrm{i}\hat{a}_-)}, \quad z \in \mathbb{C}, \tag{2.20}$$

where $\mathrm{Re}z^{1/2}, \mathrm{Re}(z-2\mathrm{i})^{1/2} \geq 0$ and $\hat{a}_{\pm} = 1 \mp \sqrt{1-\beta^{*2}}$, as before, with $\mathrm{Re}\sqrt{1-\beta^{*2}} \geq 0$. Then $F(z)$ has simple poles at $z = \mathrm{i}\hat{a}_+$ (which may lie near the real axis if $\mathrm{Re}\hat{a}_+$ is small), and $z = \mathrm{i}\hat{a}_-$ (which cannot lie near the real axis as $\mathrm{Re}\hat{a}_- \geq 1$). Recalling (2.10) we then have, at least provided $\mathrm{Re}\hat{a}_+ \neq 0$ or $\mathrm{Im}\hat{a}_+ > 0$, so that the pole at $\mathrm{i}\hat{a}_+$ does not lie on the positive real axis,

$$|\check{\kappa}_{\beta^*}^{(m)}(s)| \leq \frac{1}{\pi}\left|\int_0^{\infty} F(r) r^m \mathrm{e}^{-rs}\,\mathrm{d}r\right| + \left|C_{\beta^*}\hat{a}_+^m \mathrm{e}^{\mathrm{Im}\hat{a}_+ s}\right|, \quad s > 0. \tag{2.21}$$

Now, since $\mathrm{Re}\beta^* \geq \epsilon$, it is easy to see that $\mathrm{Im}\hat{a}_+ = 0$ if and only if $\beta^* \in [\epsilon, 1]$, and in this case $\mathrm{Re}\hat{a}_+ \geq 1 - \sqrt{1-\epsilon^2} = \epsilon^2/(1+\sqrt{1-\epsilon^2}) > \epsilon^2/2$. We thus define $S_\epsilon := \{\beta^* : \mathrm{Re}\beta^* \geq \epsilon, |\beta^*| \leq \epsilon^{-1}, \mathrm{Re}\hat{a}_+ \leq \epsilon^2/4\}$. Then S_ϵ is closed and bounded, and $|\mathrm{Im}\hat{a}_+|$ and $|\sqrt{1-\beta^{*2}}|$ are both continuous and non-zero on S_ϵ. Thus, for some $\eta > 0$,

$$|\mathrm{Im}\hat{a}_+| \geq \eta \quad \text{and} \quad \left|\sqrt{1-\beta^{*2}}\right| \geq \eta, \tag{2.22}$$

for all $\beta^* \in S_\epsilon$.

Next, we note that if $\mathrm{Re}\hat{a}_+ > 0$ then $C_{\beta^*} = 0$ while if $\mathrm{Re}\hat{a}_+ \leq 0$ then $\beta^* \in S_\epsilon$ so that (2.22) holds. Moreover, if $C_{\beta^*} \neq 0$ then $\mathrm{Im}\beta^* < 0$ and so $\mathrm{Im}\hat{a}_+ < 0$. Since also $|\hat{a}_{\pm}| \leq 1 + \sqrt{1+\epsilon^{-2}}$, we see that

$$\left|C_{\beta^*}\hat{a}_+^m \mathrm{e}^{\mathrm{Im}\hat{a}_+ s}\right| \leq C_\epsilon \mathrm{e}^{-\eta s}, \quad s > 0.$$

We turn to bounding the first term on the right hand side of (2.21). To do this we consider the two cases $|\mathrm{Re}\hat{a}_+| > \epsilon^2/4$ and $|\mathrm{Re}\hat{a}_+| \leq \epsilon^2/4$ separately.

First, suppose $|\mathrm{Re}\hat{a}_+| > \epsilon^2/4$. Then

$$|F(r)| \leq C_\epsilon r^{1/2}, \quad r > 0, \tag{2.23}$$

and thus

$$\left|\int_0^{\infty} F(r) r^m \mathrm{e}^{-rs}\,\mathrm{d}r\right| \leq C_\epsilon \int_0^{\infty} r^{m+1/2}\mathrm{e}^{-rs}\,\mathrm{d}r \leq C_\epsilon \Gamma(m+3/2) s^{-m-3/2}, \quad s > 0, \tag{2.24}$$

where Γ is the Gamma function (see eg. [2, (6.1.1)]). This bound suffices when $s > 1$, but for $0 < s \le 1$ we need a sharper bound.

We proceed by establishing bounds on the m^{th} derivatives of the first two terms on the right hand side of (2.8), for $0 < s \le 1$. It can easily be deduced from the power series representations for the Bessel functions (eg. [2]) that there exist constants C_j, $j = 0, \ldots$, such that, for $0 < z \le 1$,

$$|H_0^{(1)}(z)| \le C_0(1 + |\log z|), \tag{2.25}$$

$$\left|\frac{d^m}{dz^m} H_0^{(1)}(z)\right| \le C_m z^{-m}, \quad m = 1, 2, \ldots. \tag{2.26}$$

Next note that, for $0 < s \le 1$, the m^{th} derivative of the second term in (2.8) has absolute value not more than

$$\left|\frac{\beta^{*2}}{\pi} \int_0^\infty \frac{(\mathrm{i} - t)^m \mathrm{e}^{-st} t^{-1/2}\,\mathrm{d}t}{(t - 2\mathrm{i})^{1/2}(t^2 - 2\mathrm{i}t - \beta^{*2})}\right| \le \frac{\epsilon^{-2}}{\pi} \int_0^\infty \frac{(1 + t^2)^{m/2} \mathrm{e}^{-st} t^{-1/2}\,\mathrm{d}t}{(t^2 + 4)^{1/4}\,|(t - \mathrm{i}\hat{a}_+)(t - \mathrm{i}\hat{a}_-)|} \tag{2.27}$$

$$\le C_\epsilon \left[\int_0^1 t^{-1/2}\,\mathrm{d}t + \int_1^\infty t^{m-1} \mathrm{e}^{-st}\,\mathrm{d}t\right] \tag{2.28}$$

$$\le \begin{cases} C_\epsilon(1 - \log s), & m = 0, \\ C_\epsilon(1 + \Gamma(m)) s^{-m}, & m = 1, 2, \ldots. \end{cases} \tag{2.29}$$

Combining (2.25), (2.26) and (2.29) and recalling (2.9) the result follows.

Now we consider the case $0 \le \mathrm{Re}\hat{a}_+ \le \epsilon^2/4$ (the proof for the case $-\epsilon^2/4 \le \mathrm{Re}\hat{a}_+ < 0$ is similar). As $\beta \in S_\epsilon$, (2.22) holds. If $\mathrm{Im}\hat{a}_+ > 0$ then the bounds (2.23) and (2.28) hold and we proceed as above. If $\mathrm{Im}\hat{a}_+ < 0$ however, $F(z)$ has a pole at $z = \mathrm{i}\hat{a}_+$ with $\mathrm{Re}(\mathrm{i}\hat{a}_+) > \eta$, $0 \le \mathrm{Im}(\mathrm{i}\hat{a}_+) \le \epsilon^2/4$. To bound the integrals on the left hand side of (2.24) and (2.27) in this case uniformly in β^* we first deform the path of integration. Define Γ_ϵ to be the semicircle, centre $(-\mathrm{Im}\hat{a}_+, 0)$, radius $\tilde{\eta} := \min(1/2, \eta)$, lying in the lower half plane. (Note that by (2.22) $\mathrm{Re}z > \eta/2$ for $z \in \Gamma_\epsilon$.) Let $\gamma_\epsilon = [0, -\mathrm{Im}\hat{a}_+ - \eta/2] \cup [-\mathrm{Im}\hat{a}_+ + \eta/2, \infty)$. Then, by Cauchy's theorem, it follows from (2.21) that, for $\mathrm{Re}\hat{a}_+ > 0$,

$$|\check{\kappa}_{\beta^*}^{(m)}(s)| \le \frac{1}{\pi}\left|\int_{\gamma_\epsilon} F(r) r^m \mathrm{e}^{-rs}\,\mathrm{d}r + \int_{\Gamma_\epsilon} F(r) r^m \mathrm{e}^{-rs}\,\mathrm{d}r\right|, \quad s > 0. \tag{2.30}$$

By continuity arguments, taking the limit $\mathrm{Re}\hat{a}_+ \to 0^+$ in (2.30), equation (2.30) holds also for $\mathrm{Re}\hat{a}_+ = 0$. For $r \in \gamma_\epsilon$ the bound (2.23) holds, and so the integral over γ_ϵ is bounded by the right hand side of (2.24). Further,

$$\left|\int_{\Gamma_\epsilon} F(r) r^m \mathrm{e}^{-rs}\,\mathrm{d}r\right| \le \frac{\pi\eta}{2} \max_{r \in \Gamma_\epsilon} |F(r) r^m \mathrm{e}^{-rs}| \le C_\epsilon \mathrm{e}^{-\eta s/2},$$

so we obtain the required bound for $s \ge 1$. To obtain the desired bound for $0 < s \le 1$ we proceed as in the case $|\mathrm{Re}\hat{a}_+| > \epsilon^2/4$, but deforming the path of integration as above to bound the left hand side of (2.27). □

The following result is a slight sharpening of [12, theorem 2.6], obtained by combining the bounds in lemma 2.2 and (2.12) with the representations (2.17) and (2.18).

THEOREM 2.3. *Suppose (1.4) holds for some $\epsilon > 0$. Then, for $r > 0$, $j = 1, \ldots, n$, $m = 0, 1, \ldots$, there exist constants c_m, dependent only on m and ϵ, such that*

$$\left|f_j^{\pm(m)}(r)\right| \le c_m \cos\theta E_m(r),$$

where

$$E_m(r) = \begin{cases} 1, & m = 0, \\ 1 - \log r, & m = 1, \\ r^{1-m}, & m \geq 2, \end{cases} \qquad \text{for } 0 < r \leq 1,$$
$$E_m(r) = r^{-\frac{1}{2}-m}, \qquad \text{for } r > 1.$$

Remark. Using the identical argument it can easily be shown that $|f_{n+1}^{+}{}^{(m)}(r)|$, $|f_0^{-(m)}(r)| \leq c_m \cos\theta E_m(r)$, $r > 0$, for $m = 0, 1, \ldots$, where c_m is the same constant as in theorem 2.3.

The design of our numerical scheme is based on the following sharper bound on $|f_j^{\pm}(r)|$ when $r > 1$.

THEOREM 2.4. *Suppose (1.4) holds for some $\epsilon > 0$. Then for $r > 1$, $j = 0, \ldots, n$,*

$$\left|f_{j+1}^{+}(r)\right|, \left|f_j^{-}(r)\right| \leq C_\epsilon \frac{r^{-3/2} n^3}{\cos\theta}.$$

Proof. First we consider $f_j^{-}(r)$. Recalling (2.14), for $j = 0, \ldots, n$, $f_j^{-}(r) = I_1(r) + I_2(r)$, where

$$I_1(r) := \int_{\tilde{t}_j}^{\infty} \check{\kappa}_{\beta_j}(t - \tilde{t}_j + r) \mathrm{e}^{\mathrm{i}t} \mathrm{i}(\beta(t/k) - \beta_j) \Psi(t)\, \mathrm{d}t,$$
$$I_2(r) := \int_{\tilde{t}_j}^{\infty} \check{\kappa}_{\beta_j}(t - \tilde{t}_j + r) \mathrm{e}^{\mathrm{i}t} \mathrm{i}(\beta(t/k) - \beta_j) \Phi(t)\, \mathrm{d}t.$$

We begin by establishing a bound on I_1. Recalling (2.13) and (2.7),

$$I_1(r) = \sum_{m=j+1}^{n} \mathrm{i}(\beta_m - \beta_j) \int_{\tilde{t}_{m-1}}^{\tilde{t}_m} \check{\kappa}_{\beta_j}(t - \tilde{t}_j + r)(1 + R_{\beta_m}(\theta)) \mathrm{e}^{\mathrm{i}t(\sin\theta + 1)}\, \mathrm{d}t$$
$$+ \mathrm{i}(\beta_c - \beta_j) \int_{\tilde{t}_n}^{\infty} \check{\kappa}_{\beta_j}(t - \tilde{t}_j + r)(1 + R_{\beta_c}(\theta)) \mathrm{e}^{\mathrm{i}t(\sin\theta + 1)}\, \mathrm{d}t.$$

Integrating by parts,

$$I_1(r) = \sum_{m=j+1}^{n} \frac{(\beta_m - \beta_j)(1 + R_{\beta_m}(\theta))}{\sin\theta + 1} \left(\left[\check{\kappa}_{\beta_j}(t - \tilde{t}_j + r) \mathrm{e}^{\mathrm{i}t(\sin\theta+1)} \right]_{\tilde{t}_{m-1}}^{\tilde{t}_m} \right.$$
$$\left. - \int_{\tilde{t}_{m-1}}^{\tilde{t}_m} \check{\kappa}'_{\beta_j}(t - \tilde{t}_j + r) \mathrm{e}^{\mathrm{i}t(\sin\theta+1)}\, \mathrm{d}t \right)$$
$$+ \frac{(\beta_c - \beta_j)(1 + R_{\beta_c}(\theta))}{\sin\theta + 1} \left(\left[\check{\kappa}_{\beta_j}(t - \tilde{t}_j + r) \mathrm{e}^{\mathrm{i}t(\sin\theta+1)} \right]_{\tilde{t}_n}^{\infty} \right.$$
$$\left. - \int_{\tilde{t}_n}^{\infty} \check{\kappa}'_{\beta_j}(t - \tilde{t}_j + r) \mathrm{e}^{\mathrm{i}t(\sin\theta+1)}\, \mathrm{d}t \right).$$

Now from lemma 2.2, for $r > 1$

$$\left|\check{\kappa}_{\beta_j}(\tilde{t}_m - \tilde{t}_j + r)\right| \leq C_\epsilon (\tilde{t}_m - \tilde{t}_j + r)^{-3/2} \leq C_\epsilon r^{-3/2}, \quad m = j, \ldots, n.$$

Thus, noting that $|1+R_{\beta_m}(\theta)| = |2\cos\theta/(\cos\theta+\beta_m)| \le C_\epsilon \cos\theta$ and $|\beta_m - \beta_j| \le 2/\epsilon$, and using lemma 2.2 again to bound $\check{\kappa}'_{\beta_j}$, we have, for $r > 1$,

$$|I_1(r)| \le C_\epsilon \frac{(n+1-j)\cos\theta}{\sin\theta+1}\left[r^{-3/2} + \int_{\tilde{t}_j}^{\infty} \left|\check{\kappa}'_{\beta_j}(t-\tilde{t}_j+r)\right| \,\mathrm{d}t\right]$$

$$\le C_\epsilon \frac{r^{-3/2} n\cos\theta}{\sin\theta+1}. \tag{2.31}$$

It now remains to establish a bound on I_2. Recalling (2.16) and (2.19),

$$|I_2(r)| \le 2\epsilon \left(J_\infty^+ + \sum_{m=j+1}^{n} (J_m^+ + J_m^-)\right), \tag{2.32}$$

where

$$J_m^+ := \int_{\tilde{t}_{m-1}}^{\tilde{t}_m} |\check{\kappa}_{\beta_j}(t-\tilde{t}_j+r)||f_m^+(t-\tilde{t}_{m-1})|\,\mathrm{d}t, \tag{2.33}$$

$$J_m^- := \int_{\tilde{t}_{m-1}}^{\tilde{t}_m} |\check{\kappa}_{\beta_j}(t-\tilde{t}_j+r)||f_m^-(\tilde{t}_m-t)|\,\mathrm{d}t, \tag{2.34}$$

$$J_\infty^+ := \int_{\tilde{t}_n}^{\infty} |\check{\kappa}_{\beta_j}(t-\tilde{t}_j+r)||f_{n+1}^+(t-\tilde{t}_n)|\,\mathrm{d}t. \tag{2.35}$$

First we bound J_∞^+. Applying lemma 2.2 and theorem 2.3, and noting the remark after theorem 2.3, for $r > 1$,

$$\begin{aligned} J_\infty^+ &\le C_\epsilon \cos\theta \int_{\tilde{t}_n}^{\infty} (t-\tilde{t}_n+r)^{-3/2}(1+t-\tilde{t}_n)^{-1/2}\,\mathrm{d}t \\ &= C_\epsilon \cos\theta \int_0^{\infty} (s+r)^{-3/2}(1+s)^{-1/2}\,\mathrm{d}s \\ &\le C_\epsilon \cos\theta \left(r^{-3/2}\int_0^r (1+s)^{-1/2}\,\mathrm{d}s + r^{-1/2}\int_r^\infty (s+r)^{-3/2}\,\mathrm{d}s\right) \\ &\le C_\epsilon r^{-1}\cos\theta. \end{aligned}$$

Arguing similarly, $J_m^+ \le C_\epsilon r^{-1}\cos\theta$, but to bound J_m^- we need a slightly different argument. Again using lemma 2.2 and theorem 2.3 we have

$$\begin{aligned} J_m^- &\le C_\epsilon \cos\theta \int_{\tilde{t}_{m-1}}^{\tilde{t}_m} (t-\tilde{t}_{m-1}+r)^{-3/2}(1+\tilde{t}_m-t)^{-1/2}\,\mathrm{d}t \\ &= C_\epsilon \cos\theta \int_0^{2D} (s+r)^{-3/2}(1+2D-s)^{-1/2}\,\mathrm{d}s, \end{aligned}$$

with $D := (\tilde{t}_m - \tilde{t}_{m-1})/2$. Splitting the integral,

$$\begin{aligned} J_m^- &\le C_\epsilon \cos\theta \left[(1+D)^{-1/2}\int_0^D (s+r)^{-3/2}\,\mathrm{d}s + (D+r)^{-3/2}\int_D^{2D}(1+2D-s)^{-1/2}\,\mathrm{d}s\right] \\ &\le C_\epsilon \cos\theta \left[(1+D)^{-1/2}\frac{((D+r)^{1/2}-r^{1/2})}{r^{1/2}(D+r)^{1/2}} + (D+r)^{-3/2}\int_0^D (1+t)^{-1/2}\,\mathrm{d}t\right] \end{aligned}$$

$$\leq C_\epsilon \cos\theta \left[\frac{(1+D)^{-1/2}}{r^{1/2}(D+r)^{1/2}} \frac{(D+r-r)}{((D+r)^{1/2}+r^{1/2})} + (D+r)^{-3/2}(1+D)^{1/2} \right]$$
$$\leq C_\epsilon r^{-1} \cos\theta.$$

Thus, recalling (2.32), $|I_2(r)| \leq C_\epsilon r^{-1} n \cos\theta$. Combining this with (2.31), we have shown that for $r > 1$, $j = 0, \ldots, n$,

$$|f_j^-(r)| \leq |I_1(r)| + |I_2(r)| \leq C_\epsilon r^{-1} n \cos\theta \left(\frac{r^{-1/2}}{1+\sin\theta} + 1 \right). \tag{2.36}$$

Proceeding in a similar way, we can show that, for $r > 1$, $j = 1, \ldots, n+1$,

$$|f_j^+(r)| \leq C_\epsilon r^{-1} n \cos\theta \left(\frac{r^{-1/2}}{1-\sin\theta} + 1 \right). \tag{2.37}$$

Recalling (2.32)–(2.35), we can use (2.36) and (2.37) to establish sharper bounds on I_2. Using (2.37) in (2.35), we have for $r > 1$ that

$$\begin{aligned} J_\infty^+ &\leq C_\epsilon n \cos\theta \int_{\tilde{t}_n}^\infty (t - \tilde{t}_n + r)^{-3/2} (1 + t - \tilde{t}_n)^{-1} \left(1 + \frac{(1+t-\tilde{t}_n)^{-1/2}}{1-\sin\theta} \right) \mathrm{d}t \\ &= C_\epsilon n \cos\theta \int_0^\infty (s+r)^{-3/2} (1+s)^{-1} \left(1 + \frac{(1+s)^{-1/2}}{1-\sin\theta} \right) \mathrm{d}s \\ &\leq C_\epsilon n \cos\theta \left(r^{-3/2} \int_0^r (1+s)^{-1} \left(1 + \frac{(1+s)^{-1/2}}{1-\sin\theta} \right) \mathrm{d}s \right. \\ &\qquad \left. + r^{-1} \int_r^\infty (s+r)^{-3/2} \left(1 + \frac{r^{-1/2}}{1-\sin\theta} \right) \mathrm{d}s \right) \\ &\leq C_\epsilon r^{-3/2} n \cos\theta (\log r + (1-\sin\theta)^{-1}). \end{aligned} \tag{2.38}$$

Arguing similarly, we can show that

$$J_m^+ \leq C_\epsilon r^{-3/2} n \cos\theta (\log r + (1-\sin\theta)^{-1}), \quad m = j+1, \ldots, n, \tag{2.39}$$

but again for J_m^- we must argue differently. Using (2.36) and lemma 2.2

$$\begin{aligned} J_m^- &\leq C_\epsilon n \cos\theta \int_{\tilde{t}_{m-1}}^{\tilde{t}} (t - \tilde{t}_{m-1} + r)^{-3/2} (1 + \tilde{t}_m - t)^{-1} \left(1 + \frac{(1+\tilde{t}_m - t)^{-1/2}}{1+\sin\theta} \right) \mathrm{d}t \\ &\leq C_\epsilon n \cos\theta \int_0^{2D} (s+r)^{-3/2} (1+2D-s)^{-1} \left(1 + \frac{(1+2D-s)^{-1/2}}{1+\sin\theta} \right) \mathrm{d}s, \end{aligned}$$

with $D := (\tilde{t}_m - \tilde{t}_{m-1})/2$ as before. Splitting the integral as above

$$\begin{aligned} J_m^- \leq C_\epsilon n \cos\theta \left[(1+D)^{-1} \left(1 + \frac{(1+D)^{-1/2}}{1+\sin\theta} \right) \int_0^D (s+r)^{-3/2} \, \mathrm{d}s \right. \\ \left. + (D+r)^{-3/2} \int_0^D (1+t)^{-1} \left(1 + \frac{(1+t)^{-1/2}}{1+\sin\theta} \right) \mathrm{d}t \right]. \end{aligned} \tag{2.40}$$

Considering first the first term on the right hand side

$$(1+D)^{-1} \left(1 + \frac{(1+D)^{-1/2}}{1+\sin\theta} \right) \int_0^D (s+r)^{-3/2} \, \mathrm{d}s$$

$$\leq C(1+D)^{-1}\left(1+\frac{(1+D)^{-1/2}}{1+\sin\theta}\right)\frac{((D+r)^{1/2}-r^{1/2})}{r^{1/2}(D+r)^{1/2}}$$
$$\leq \frac{D}{(1+D)(D+r)^{1/2}}\frac{1}{r^{1/2}(D+r)^{1/2}}\left(1+\frac{(1+D)^{-1/2}}{1+\sin\theta}\right)$$
$$\leq Cr^{-3/2}(1+\sin\theta)^{-1}. \tag{2.41}$$

To bound the second term, we need to consider the cases $r \geq D$ and $r < D$ separately. If $r \geq D$, we have

$$(D+r)^{-3/2}(\log(1+D)+(1+\sin\theta)^{-1}) \leq Cr^{-3/2}(\log r+(1+\sin\theta)^{-1}). \tag{2.42}$$

If $r < D$ then we need to split the integral a second time to get

$$(D+r)^{-3/2}\left[\int_0^r \frac{1}{1+t}\left(1+\frac{(1+t)^{-1/2}}{1+\sin\theta}\right)\,\mathrm{d}t+\int_r^D \frac{1}{1+t}\left(1+\frac{(1+t)^{-1/2}}{1+\sin\theta}\right)\,\mathrm{d}t\right]$$
$$\leq C(D+r)^{-3/2}\left[\log r(1+\sin\theta)^{-1}+(D-r)(1+r)^{-1}(1+\sin\theta)^{-1}\right]$$
$$\leq C\left[r^{-3/2}\log r+\frac{D-r}{(D+r)^{3/2}(1+r)}\right](1+\sin\theta)^{-1}$$
$$\leq Cr^{-3/2}\log r(1+\sin\theta)^{-1}. \tag{2.43}$$

Putting (2.41), (2.42) and (2.43) into (2.40) we get

$$J_m^- \leq C_\epsilon r^{-3/2} n\cos\theta(\log r+1)(1+\sin\theta)^{-1},$$

and thus, combining with (2.38) and (2.39),

$$|I_2(r)| \leq C_\epsilon r^{-3/2}n^2\cos\theta(\log r+1)(1-\sin^2\theta)^{-1} = C_\epsilon\frac{r^{-3/2}(\log r+1)n^2}{\cos\theta}.$$

Thus

$$|f_j^-(r)| \leq |I_1|+|I_2| \leq C_\epsilon\frac{r^{-3/2}(\log r+1)n^2}{\cos\theta}, \tag{2.44}$$

and in a similar way it can be proved that

$$|f_j^+(r)| \leq C_\epsilon\frac{r^{-3/2}(\log r+1)n^2}{\cos\theta}. \tag{2.45}$$

To remove the dependence on $\log r$ in (2.44), (2.45), we use the fact that $\int_0^\infty |f_j^\pm(r)|\,\mathrm{d}r$ is now bounded by a constant, namely

$$\int_0^\infty |f_j^\pm(r)|\,\mathrm{d}r \leq C_\epsilon\frac{n^2}{\cos\theta},$$

using (2.44), (2.45). Using this fact, and lemma 2.2,

$$J_m^\pm \leq C_\epsilon r^{-3/2}\int_0^\infty |f_m^\pm(s)|\,\mathrm{d}s \leq C_\epsilon\frac{r^{-3/2}n^2}{\cos\theta},$$

and an identical bound holds on J_∞^+. Hence, recalling (2.32),

$$|I_2(r)| \leq C_\epsilon\frac{r^{-3/2}n^3}{\cos\theta},$$

and combining this with (2.31) the result follows. □

3. Galerkin method and error analysis. Our aim now is to design a numerical method for the solution of (2.15), supported by a full error analysis, for which the error bounds are independent of the parameter $k(b-a)$. To achieve this we will work in $L_2(\mathbb{R})$, and to that end we introduce the operator $Q : L_\infty(\mathbb{R}) \to L_2(\mathbb{R})$ defined by

$$Q\chi(s) := \begin{cases} \chi(s), & s \in [\tilde{a}, \tilde{b}] = [\tilde{t}_0, \tilde{t}_n], \\ 0, & s \in \mathbb{R}\backslash[\tilde{a}, \tilde{b}]. \end{cases}$$

Writing $\Phi^* := Q\Phi$, and noting that $K_\beta^{\beta_c}\Phi = K_\beta^{\beta_c}\Phi^*$, it follows from (2.15) that

$$\Phi^* - QK_\beta^{\beta_c}\Phi^* = Q\Psi_\beta^{\beta_c}, \tag{3.1}$$

where Φ^* and $Q\Psi_\beta^{\beta_c}$ are both in $L_2(\mathbb{R})$.

Existence and boundedness of $(I - QK_\beta^{\beta_c})^{-1} : L_2(\mathbb{R}) \to L_2(\mathbb{R})$ are shown in [12], where it is also shown that the unique solution $\Phi^* = (I - QK_\beta^{\beta_c})^{-1}Q\Psi_\beta^{\beta_c}$ of (3.1) satisfies $\|\Phi^*\|_2 \le C_1\|Q\Psi_\beta^{\beta_c}\|_2$, with $C_1 = \mathrm{Re}\beta_c/(\mathrm{Re}\beta_c - \|\beta - \beta_c\|_\infty)$ if

$$|\beta_j - \beta_c| < \mathrm{Re}\beta_c, \quad j = 1, \ldots, n, \tag{3.2}$$

and C_1 unspecified but dependent only on ϵ and β_c if (3.2) does not hold.

To approximate the solution $\Phi^* = Q\Phi$ of (3.1) we use a Galerkin method, similar to that in [12], but with the approximation space chosen in a different way so as to take advantage of our stronger bound on Φ (theorem 2.4), in order to remove the dependence of the error estimates on $k(b-a)$. As in [12], on each interval $(\tilde{t}_{j-1}, \tilde{t}_j)$, we approximate $f_j^+(s - \tilde{t}_{j-1})$ and $f_j^-(\tilde{t}_j - s)$ in (2.16) by conventional piecewise polynomial approximations, rather than approximating Φ itself. This makes sense since, as quantified by theorems 2.3 and 2.4, the functions $f_j^+(s - \tilde{t}_{j-1})$ and $f_j^-(\tilde{t}_j - s)$ are smooth (their higher order derivatives are small) away from $\tilde{t}_{j-1}$ and $\tilde{t}_j$, respectively. To approximate $f_j^+(s - \tilde{t}_{j-1})$ and $f_j^-(\tilde{t}_j - s)$ we use piecewise polynomials of a fixed degree $\nu \ge 0$ on a graded mesh, the mesh grading adapted in an optimal way to the bounds on $f_j^{\pm(m)}$ in theorems 2.3 and 2.4.

To begin, we define a graded mesh on a general interval $[0, A]$, for $A > 1$, with more mesh points near 0 and less near A. This mesh is identical to that defined in [12, definition 3.1]; the difference here is in how we choose the value of A when we apply this mesh to the discretisation of each interval $[\tilde{t}_{j-1}, \tilde{t}_j]$. Whereas in [12], A was chosen as a function of $\tilde{t}_{j-1}$ and $\tilde{t}_j$ and the functions $f_j^\pm$ were approximated over the whole interval $[\tilde{t}_{j-1}, \tilde{t}_j]$, here we choose A as a function of N, a positive integer, where the size of N also determines the density of the mesh on $[0, A]$. A judicious choice of $A = A(N)$, as described below, allows us to discretise only a subsection of the interval $[\tilde{t}_{j-1}, \tilde{t}_j]$ near to $\tilde{t}_{j-1}$ and $\tilde{t}_j$, and to approximate $f_j^\pm$ by zero away from these points without harming the overall accuracy of our scheme. This is the key to achieving error estimates independent of $k(b-a)$.

The mesh we use also has similarities to that used in [24] for solving (1.1) in the case $k = \mathrm{i}\tau$, $\tau > 0$, τ large, where a similar idea of only discretising a subsection of the boundary as $k \to \infty$ was used in order to establish error bounds independent of τ.

DEFINITION 3.1. *For $A > 1$ and $N = 2, 3, \ldots$, the mesh $\Lambda_{N,A} = \{y_0, \ldots, y_{N+N_A}\}$ consists of the points $y_i = (i/N)^q$, $i = 0, \ldots, N$, where $q = 1 + 2\nu/3$, together with the points $y_{N+j} = A^{j/N_A}$, $j = 1, \ldots, N_A$, where $N_A = \lceil N^* \rceil$, the smallest integer $\ge N^*$, and $N^* := -\log A/[q\log(1 - 1/N)]$.*

The mesh $\Lambda_{N,A}$ is a composite mesh with a polynomial grading on $[0,1]$ and a geometric grading on $[1,A]$. The definition of N_A ensures a smooth transition between the two parts of the mesh. Precisely, the definition of N^* is such that, in the case $N_A = N^*$, it holds that $y_{N+1}/y_N = y_N/y_{N-1}$, so that y_{N-1} and y_N are points in both the polynomial and the geometric parts of the mesh. It is shown in [12] that the total number of subintervals $N + N_A$ of the mesh on $[0,A]$ satisfies

$$N + N_A < \left(\frac{3}{2} + \frac{\log A}{q}\right) N. \tag{3.3}$$

Let $\Pi_{A,N,\nu} := \{\sigma : \sigma|_{[y_{j-1},y_j]} \text{ is a polynomial of degree} \le \nu,\ j = 1,\dots,N+N_A\}$, and let P_N^* be the orthogonal projection operator from $L_2(0,A)$ to $\Pi_{A,N,\nu}$, so that setting $p = P_N^* f$ minimises $\|f-p\|_{2,(0,A)} = \{\int_0^A |f(t)-p(t)|^2\,\mathrm{d}t\}^{1/2}$ over all $p \in \Pi_{A,N,\nu}$. The mesh $\Lambda_{N,A}$ is designed to approximately minimise $\|f - P_N^* f\|_{2,(0,A)}$, over all meshes with the same number of points, when $f \in \mathcal{C}^\infty(0,\infty)$ with $|f^{(\nu+1)}(s)| = E_{\nu+1}(s)$, $s > 0$, where $E_{\nu+1}$ is defined as in theorem 2.3. It achieves this by ensuring that $\|f - P_N^* f\|_{2,(y_{j-1},y_j)}$ is approximately constant for $j = 1,\dots,N+N_A$, i.e. by equidistributing the approximation error over the intervals of the mesh, as shown in the proof of the following result in [12].

THEOREM 3.2. *Suppose that $f \in \mathcal{C}^\infty(0,\infty)$ and $|f'(s)| \le E_1(s)$, $|f^{(\nu+1)}(s)| \le E_{\nu+1}(s)$, $s > 0$. Then there exists a constant C_ν depending only on ν such that*

$$\|f - P_N^* f\|_{2,(0,A)} \le C_\nu \frac{1 + \log^{1/2} A}{N^{\nu+1}}.$$

To form our approximation space on $[\tilde a, \tilde b] = [\tilde t_0, \tilde t_n]$, we begin by defining

$$A_j := \min\left\{\alpha \frac{n^3 N^{\nu+1}}{\cos\theta}, \tilde t_j - \tilde t_{j-1}\right\}, \tag{3.4}$$

where $\alpha \ge 1$ is an absolute constant which will be determined experimentally and whose value will not effect the asymptotic convergence rates. The reason for our choice of A_j will become apparent shortly, in the proof of theorem 3.3. Clearly A_j is bounded independently of $k(b-a)$. As we are primarily concerned with the high frequency problem, we assume for simplicity that $A_j \ge 1$, $j = 1,\dots,n$, but remark that in the case $A_j < 1$ for any value of j then we can define Λ_{N,A_j} to be an appropriate subset of the points y_i, and this will give similar approximation properties to those achieved using Λ_{N,A_j} when $A_j \ge 1$. For $j = 1,\dots,n$ we define the two meshes $\Omega_j^+ := \tilde t_{j-1} + \Lambda_{N,A_j}$, $\Omega_j^- := \tilde t_j - \Lambda_{N,A_j}$. Letting $e_\pm(s) := \mathrm{e}^{\pm \mathrm{i}s}$, $s \in \mathbb{R}$, we then define $V_{\Omega_j^+,\nu} := \{\sigma e_+ : \sigma \in \Pi_{\Omega_j^+,\nu}\}$, $V_{\Omega_j^-,\nu} := \{\sigma e_- : \sigma \in \Pi_{\Omega_j^-,\nu}\}$, for $j = 1,\dots,n$, where

$$\begin{aligned}
\Pi_{\Omega_j^+,\nu} := \{&\sigma \in L_2(\mathbb{R}) : \sigma|_{(\tilde t_{j-1}+y_{m-1},\tilde t_{j-1}+y_m)} \text{ is a polynomial of degree} \le \nu, \text{ for}\\
&m = 1,\dots,N+N_{A_j}, \text{ and } \sigma|_{\mathbb{R}\setminus[\tilde t_{j-1},\tilde t_{j-1}+A_j]} = 0\},\\
\Pi_{\Omega_j^-,\nu} := \{&\sigma \in L_2(\mathbb{R}) : \sigma|_{(\tilde t_j - y_m,\tilde t_j - y_{m-1})} \text{ is a polynomial of degree} \le \nu, \text{ for}\\
&m = 1,\dots,N+N_{A_j}, \text{ and } \sigma|_{\mathbb{R}\setminus[\tilde t_j - A_j,\tilde t_j]} = 0\},
\end{aligned}$$

and $y_0,\dots,y_{N_{A_j}}$ are the points of the mesh Λ_{N,A_j}. Our approximation space is then $V_{\Omega,\nu}$, the linear span of $\bigcup_{j=1,\dots,n}\{V_{\Omega_j^+,\nu} \cup V_{\Omega_j^-,\nu}\}$.

Let $(\cdot,\cdot)$ denote the usual inner product on $L_2(\mathbb{R})$, $(\chi_1,\chi_2) := \int_{-\infty}^{\infty} \chi_1(s)\overline{\chi_2}(s)\,\mathrm{d}s$, $\chi_1,\chi_2 \in L_2(\mathbb{R})$. Then our Galerkin method approximation, $\Phi_N \in V_{\Omega,\nu}$, is defined by

$$(\Phi_N,\rho) = (\Psi_\beta^{\beta_c},\rho) + (K_\beta^{\beta_c}\Phi_N,\rho), \qquad \text{for all } \rho \in V_{\Omega,\nu}; \tag{3.5}$$

equivalently,

$$\Phi_N - P_N K_\beta^{\beta_c}\Phi_N = P_N Q \Psi_\beta^{\beta_c}, \tag{3.6}$$

where $P_N : L_2(\mathbb{R}) \to V_{\Omega,\nu}$ is the operator of orthogonal projection onto $V_{\Omega,\nu}$. Equation (3.5) can be written explicitly as a system of M_N linear algebraic equations, where M_N, the dimension of $V_{\Omega,\nu}$, i.e. the number of degrees of freedom, is given by

$$M_N = 2(\nu+1)\sum_{j=1}^{n}(N + N_{A_j}). \tag{3.7}$$

By (3.3) and (3.4)

$$M_N < 2(\nu{+}1)\sum_{j=1}^{n}\left(\frac{3}{2}+\frac{\log A_j}{q}\right)N \le 2(\nu{+}1)nN\left(\frac{3}{2}+\frac{\log(\alpha n^3/\cos\theta)+(\nu{+}1)\log N}{q}\right).$$

Using a similar argument to that for the Galerkin method in [12], it can be shown that (3.6) is uniquely solvable and that, provided (3.2) holds,

$$\|(I - P_N K_\beta^{\beta_c})^{-1}\| \le \frac{\mathrm{Re}\beta_c}{\mathrm{Re}\beta_c - \|\beta-\beta_c\|_\infty}, \tag{3.8}$$

and thus

$$\|\Phi^* - \Phi_N\|_2 \le \frac{\mathrm{Re}\beta_c}{\mathrm{Re}\beta_c - \|\beta-\beta_c\|_\infty}\|\Phi^* - P_N\Phi^*\|_2. \tag{3.9}$$

There is also a description in [12] of how one can perturb the original problem in such a way that the condition (3.2) on β is forced to hold, and the solution of the perturbed problem is arbitrarily close in an arbitrarily large bounded region to the solution of the original problem. In any case, numerical results in [23] suggest that the Galerkin scheme we propose is stable and convergent even when (3.2) does not hold. In this case the bound (3.9) does not apply, however.

It remains to bound $\|\Phi^* - P_N\Phi^*\|_2$, showing that our approximation space is well-adapted to approximate Φ^*. We introduce P_N^+ and P_N^-, the orthogonal projection operators from $L_2(\mathbb{R})$ onto $\Pi_{\Omega^+,\nu}$ and $\Pi_{\Omega^-,\nu}$ respectively, where $\Pi_{\Omega^\pm,\nu}$ denotes the linear span of $\bigcup_{j=1,\ldots,n}\Pi_{\Omega_j^\pm,\nu}$. We also define

$$f_+(s) := \begin{cases} f_j^+(s-\tilde t_{j-1}), & s \in (\tilde t_{j-1},\tilde t_j],\ j=1,\ldots,n,\\ 0, & s \in \mathbb{R}\backslash(\tilde t_0,\tilde t_n],\end{cases}$$

$$f_-(s) := \begin{cases} f_j^-(\tilde t_j - s), & s \in (\tilde t_{j-1},\tilde t_j],\ j=1,\ldots,n,\\ 0, & s \in \mathbb{R}\backslash(\tilde t_0,\tilde t_n].\end{cases}$$

Then we have the following error estimate.

THEOREM 3.3. *If (1.4) holds for some $\epsilon > 0$, then there exists a constant $C_{\epsilon,\nu} > 0$ such that*

$$\|f_+ - P_N^+ f_+\|_2 \le C_{\epsilon,\nu}\frac{n^{1/2}}{N^{\nu+1}}\left(1+\log^{1/2}\left(\min\left(\alpha\frac{n^3N^{\nu+1}}{\cos\theta}, k(b-a)\right)\right)\right),$$

where α is the constant in (3.4), and the identical bound holds on $\|f_- - P_N^- f_-\|_2$.

Proof. We prove the result for $\|f_+ - P_N^+ f_+\|_2$, the bound on $\|f_- - P_N^- f_-\|_2$ can be proved in a similar way. Recalling (3.4),

$$\begin{aligned}\|f_+ - P_N^+ f_+\|_2^2 &= \|f_+ - P_N^+ f_+\|_{2,(\tilde{a},\tilde{b})}^2 \\ &= \sum_{j=1}^{n} \left[\|f_+ - P_N^+ f_+\|_{2,(\tilde{t}_{j-1},\tilde{t}_{j-1}+A_j)}^2 + \|f_+ - P_N^+ f_+\|_{2,(\tilde{t}_{j-1}+A_j,\tilde{t}_j)}^2 \right].\end{aligned}$$

Now by theorems 2.3 and 3.2,

$$\|f_+ - P_N^+ f_+\|_{2,(\tilde{t}_{j-1},\tilde{t}_{j-1}+A_j)} \leq C_{\epsilon,\nu} \cos\theta \frac{1+\log^{1/2} A_j}{N^{\nu+1}}.$$

If $\alpha n^3 N^{\nu+1}/\cos\theta \geq \tilde{t}_j - \tilde{t}_{j-1}$, then $A_j = \tilde{t}_j - \tilde{t}_{j-1}$ in which case

$$\|f_+ - P_N^+ f_+\|_{2,(\tilde{t}_{j-1}+A_j,\tilde{t}_j)} = 0.$$

If $\alpha n^3 N^{\nu+1}/\cos\theta < \tilde{t}_j - \tilde{t}_{j-1}$, then $A_j = \alpha n^3 N^{\nu+1}/\cos\theta$ and then, recalling the definition of $\Pi_{\Omega^+,\nu}$ and theorem 2.4,

$$\begin{aligned}\|f_+ - P_N^+ f_+\|_{2,(\tilde{t}_{j-1}+A_j,\tilde{t}_j)}^2 &= \|f_+\|_{2,(\tilde{t}_{j-1}+A_j,\tilde{t}_j)}^2 \leq C_\epsilon^2 \frac{n^6}{\cos^2\theta} \int_{A_j}^{\infty} s^{-3}\,\mathrm{d}s \\ &= C_\epsilon^2 \frac{n^6}{2\cos^2\theta} A_j^{-2} = \frac{C_\epsilon^2}{2\alpha^2} N^{-2(\nu+1)},\end{aligned}$$

and recalling that $\alpha \geq 1$ the result follows. □

To use the above error estimate, note from (2.16) that $\Phi^* = e_+ f_+ + e_- f_-$. But $e_+ P_N^+ f_+ + e_- P_N^- f_- \in V_{\Omega,\nu}$, and $P_N \Phi^*$ is the best approximation to Φ^* in $V_{\Omega,\nu}$. Applying theorem 3.3 we thus have that, if (1.4) holds,

$$\begin{aligned}\|\Phi^* - P_N\Phi^*\|_2 &\leq \|\Phi^* - (e_+ P_N^+ f_+ + e_- P_N^- f_-)\|_2 \\ &= \|e_+(f_+ - P_N^+ f_+) + e_-(f_- - P_N^- f_-)\|_2 \\ &\leq \|e_+\|_\infty \|f_+ - P_N^+ f_+\|_2 + \|e_-\|_\infty \|f_- - P_N^- f_-\|_2 \\ &\leq C_{\epsilon,\nu} \frac{n^{1/2}}{N^{\nu+1}} \left(1 + \log^{1/2}\left(\min\left(\alpha \frac{n^3 N^{\nu+1}}{\cos\theta}, k(b-a)\right)\right)\right).\end{aligned}$$

We have shown the following result.

THEOREM 3.4. *If (1.4) holds for some $\epsilon > 0$, then there exists a constant $C_{\epsilon,\nu} > 0$ such that*

$$\|\Phi^* - P_N\Phi^*\|_2 \leq C_{\epsilon,\nu} \frac{n^{1/2}}{N^{\nu+1}} \left(1 + \log^{1/2}\left(\min\left(\alpha \frac{n^3 N^{\nu+1}}{\cos\theta}, k(b-a)\right)\right)\right),$$

where α is the constant in (3.4).

Combining this result with the stability bound (3.9) we obtain our final error estimate for the approximation of Φ by Φ_N.

THEOREM 3.5. *If (1.4) holds for some $\epsilon > 0$, and (3.2) is satisfied, then there exists a constant $C_{\epsilon,\nu} > 0$ such that*

$$\|\Phi - \Phi_N\|_{2,(\tilde{a},\tilde{b})} = \|\Phi^* - \Phi_N\|_2 \leq \frac{C_{\epsilon,\nu} n^{1/2} (1 + \log^{1/2}(\min(\alpha n^3 N^{\nu+1}/\cos\theta, k(b-a))))}{(\mathrm{Re}\beta_c - \|\beta - \beta_c\|_\infty) N^{\nu+1}},$$

where α is the constant in (3.4). Further, the number of degrees of freedom M_N satisfies

$$M_N \leq C_{\epsilon,\nu} nN \log(\min(\alpha n^3 N^{\nu+1}/\cos\theta, k(b-a))).$$

We finish by considering the computation of an approximation to u^t throughout the upper half plane U, once the Galerkin solution Φ_N has been computed. Recalling (2.13) and (2.14) we define $\phi_N \in L_2(\tilde{a},\tilde{b})$, an approximation to ϕ on $(\tilde{a},\tilde{b})$, by

$$\phi_N(s) := \Phi_N(s) + \psi_{\beta_j}(s), \quad s \in (\tilde{t}_{j-1}, \tilde{t}_j],\ j = 1,\ldots,n,$$

where ψ_{β_j} is given explicitly by (2.7). Then, recalling that $u^t((y_1,0)) = \phi(ky_1)$, we define an approximation to u^t by replacing $u^t(y)$ by its approximation $\phi_N(ky_1)$ in (2.5), to give the approximation u_N^t defined by

$$u_N^t(x) := u_{\beta_c}^t(x) + \mathrm{i}k \int_a^b G_{\beta_c}(x,(y_1,0))(\beta(y_1)-\beta_c)\phi_N(ky_1)\,\mathrm{d}y_1. \tag{3.10}$$

From (2.2) and (2.3), and using properties of standard single-layer potentials [15], it follows that $u_N^t \in C^2(U)\cap C(\overline{U})$ and satisfies the Helmholtz equation (1.1) in U. Further, from theorem 3.5 we deduce the following error estimate.

THEOREM 3.6. *If (1.4) holds for some $\epsilon > 0$, and (3.2) is satisfied, then there exists a constant $C_{\epsilon,\nu} > 0$ such that, for $x \in \overline{U}$,*

$$|u^t(x) - u_N^t(x)| \leq \frac{C_{\epsilon,\nu} n^{1/2}(1+\log^{1/2}(\min(\alpha n^3 N^{\nu+1}/\cos\theta, k(b-a))))}{(\mathrm{Re}\beta_c - \|\beta-\beta_c\|_\infty)N^{\nu+1}},$$

where α is the constant in (3.4).

Proof. Subtracting (3.10) from (2.5) and using the Cauchy-Schwarz inequality and the definitions of Φ^* and ϕ_N, we see that

$$\begin{aligned}|u^t(x) - u_N^t(x)| &= \left|\int_{\tilde{a}}^{\tilde{b}} G_{\beta_c}(x,(t/k,0))(\beta(t/k)-\beta_c)(\Phi(t)-\Phi_N(t))\,\mathrm{d}t\right| \\ &\leq \|\beta-\beta_c\|_\infty \left\{\int_{-\infty}^{\infty} |G_{\beta_c}(x,(t/k,0))|^2\,\mathrm{d}t\right\}^{1/2} \|\Phi-\Phi_N\|_{2,(\tilde{a},\tilde{b})}.\end{aligned}$$

Now, defining $H = kx_2$, and using (2.2) we see that for $H \geq 1/2$ it holds that

$$\begin{aligned}\int_{-\infty}^{\infty} |G_{\beta_c}(x,(t/k,0))|^2\,\mathrm{d}t &\leq C_\epsilon(1+H)^2 \int_{-\infty}^{\infty} \frac{\mathrm{d}t}{(t^2+H^2)^{3/2}} \\ &= 2C_\epsilon \frac{(1+H)^2}{H^2}\int_0^\infty \frac{\mathrm{d}s}{(1+s^2)^{3/2}} \leq 18 C_\epsilon \int_0^\infty \frac{\mathrm{d}s}{(1+s^2)^{3/2}}.\end{aligned}$$

Using (2.2) and (2.3) we see that, for $0 \leq H < 1/2$,

$$\begin{aligned}\int_{-\infty}^{\infty} |G_{\beta_c}(x,(t/k,0))|^2\,\mathrm{d}t &\leq 2C_\epsilon\left(\int_{\sqrt{1-H^2}}^\infty \frac{(1+H)^2\mathrm{d}t}{(t^2+H^2)^{3/2}} + \int_0^{\sqrt{1-H^2}} (1-\frac{1}{2}\log(t^2+H^2))\,\mathrm{d}t\right) \\ &\leq 2C_\epsilon\left(\frac{9}{4}\int_{\sqrt{3}/2}^\infty \frac{\mathrm{d}t}{t^3} + \int_0^1 (1-\log t)\,\mathrm{d}t\right).\end{aligned}$$

Thus

$$|u^t(x) - u_N^t(x)| \leq C_\epsilon \|\Phi - \Phi_N\|_{2,(\tilde{a},\tilde{b})},$$

and the result follows from theorem 3.5. □

4. Implementation and numerical results. We restrict our attention in this section to the case $\nu = 0$. The implementation of the scheme is similar for higher values of ν. Recalling (3.5), the equation we wish to solve is

$$(\Phi_N, \rho) - (K_\beta^{\beta_c}\Phi_N, \rho) = (\Psi_\beta^{\beta_c}, \rho), \quad \text{for all } \rho \in V_{\Omega,0}. \tag{4.1}$$

Writing Φ_N as a linear combination of basis functions of $V_{\Omega,0}$, we have $\Phi_N(s) = \sum_{j=1}^{M_N} v_j \rho_j(s)$, where M_N is given by (3.7) and ρ_j is the j^{th} basis function, defined by

$$\rho_j(s) := \frac{\mathrm{e}^{\mathrm{i}s}\chi_{[s_{\tilde{j}}^+, s_{\tilde{j}-1}^+)}(s)}{(s_{\tilde{j}}^+ - s_{\tilde{j}-1}^+)^{1/2}}, \quad j = \tilde{j} + 2\sum_{m=1}^{p-1}(N + N_{A_m}),\ \tilde{j} = 1, \ldots, N + N_{A_p},$$

$$\rho_j(s) := \frac{\mathrm{e}^{-\mathrm{i}s}\chi_{[s_{\tilde{j}}^-, s_{\tilde{j}-1}^-)}(s)}{(s_{\tilde{j}}^- - s_{\tilde{j}-1}^-)^{1/2}}, \quad j = \tilde{j}+N+N_{A_p}+2\sum_{m=1}^{p-1}(N + N_{A_m}),\ \tilde{j} = 1, \ldots, N + N_{A_p},$$

for $p = 1, \ldots, n$, where $s_l^+ \in \Omega_p^+$, $s_l^- \in \Omega_p^-$ for $l = 0, \ldots, N + N_{A_p}$, and $\chi_{[s_1,s_2)}$ denotes the characteristic function of the interval $[s_1, s_2)$.

Equation (4.1) then becomes the linear system

$$\sum_{j=1}^{M_N} v_j((\rho_j, \rho_m) - (K_\beta^{\beta_c}\rho_j, \rho_m)) = (\Psi_\beta^{\beta_c}, \rho_m), \quad m = 1, \ldots, M_N. \tag{4.2}$$

If k is large compared to N, then, from the definition of A_j in (3.4), it is clear that the two meshes Ω_j^+ and Ω_j^- will not overlap. In this case the basis functions ρ_j, $j = 1, \ldots, M_N$, form an orthonormal basis for $V_{\Omega,\nu}$ (this is not true for the Galerkin method described in [12]), and hence the condition number of our linear system (4.2) will be bounded by (see e.g. [3, §3.6.3])

$$\begin{aligned}\|(I - P_N K_\beta^{\beta_c})\|_2 \|(I - P_N K_\beta^{\beta_c})^{-1}\|_2 &\leq (1 + \|K_\beta^{\beta_c}\|_2)\left(\frac{\mathrm{Re}\beta_c}{\mathrm{Re}\beta_c - \|\beta - \beta_c\|_\infty}\right) \\ &\leq \left(1 + \frac{\|\beta - \beta_c\|_\infty}{\mathrm{Re}\beta_c}\right)\left(\frac{\mathrm{Re}\beta_c}{\mathrm{Re}\beta_c - \|\beta - \beta_c\|_\infty}\right) \\ &= \frac{\mathrm{Re}\beta_c + \|\beta - \beta_c\|_\infty}{\mathrm{Re}\beta_c - \|\beta - \beta_c\|_\infty}, \end{aligned} \tag{4.3}$$

where we have used (3.8) (under the assumption that (3.2) holds), and the facts that $\|K_\beta^{\beta_c}\|_2 \leq \|\beta - \beta_c\|_\infty / \mathrm{Re}\beta_c$ (see e.g. [12, (3.2)]) and $\|P_N\|_2 = 1$. The fact that we can establish such a bound on the condition number of our linear system is in direct contrast to some other schemes in the literature where the approximation space consists of plane wave basis functions, e.g. [26, 28, 29], where serious difficulties due to ill-conditioning have been reported.

To evaluate the coefficients $(K_\beta^{\beta_c}\rho_j, \rho_m)$ and $(\Psi_\beta^{\beta_c}, \rho_m)$ of (4.2) we must compute some integrals numerically. The exact formulae are given in [23], but note that the most difficult of these take the forms

$$\int_0^\infty \frac{(\mathrm{i} - r)F(r)}{r(r - 2\mathrm{i})}\,\mathrm{d}r, \int_0^\infty \frac{(1 - \mathrm{e}^{rs})F(r)}{r^2}\,\mathrm{d}r, \int_0^\infty \frac{(1 - \mathrm{e}^{rs})F(r)}{r(r - 2\mathrm{i})}\,\mathrm{d}r,$$

where $s < 0$ and $F(r)$ is given by (2.20). These integrals are similar in difficulty to integral representations for the Green's function G_{β^*}, for which very efficient numerical schemes are proposed in [11]. In particular, we remark that the integrands are not oscillatory as the oscillating part of the integrands is removed by the integrations which are carried out analytically. As a result, the coefficients do not become more difficult to evaluate as $k \to \infty$.

As a numerical example, we take $\theta = \pi/4$, $n = 1$, and

$$\beta(s) = \begin{cases} 0.505 - 0.3\mathrm{i}, & s \in [-m\lambda, m\lambda], \\ 1 & s \notin [-m\lambda, m\lambda], \end{cases}$$

for m=5, 10, 20, 40, 80, 160, 320, 640, 1280, 2560 and 5120, where $k = 1$ and $\lambda = 2\pi$ is the wavelength. This experiment is equivalent to fixing the interval $[a, b] = [t_0, t_1]$ and decreasing the wavelength. The assumption (3.2) is satisfied, so that theorem 3.5 holds. For each value of m, we compute Φ_N with $\nu = 0$, $\alpha = 25\sqrt{2}$ (so that $\alpha n^3/\cos\theta = \sqrt{2}\alpha = 50$, with this value being chosen experimentally) and N=2, 4, 8, 16, 32, 64. For the purpose of computing errors, we take the "exact" solution to be the solution computed with $\sqrt{2}\alpha = 1000$ and $N = 128$. Whereas for the scheme of [12] the number of degrees of freedom needed to maintain accuracy increases logarithmically with respect to $k(b-a)$ as $k(b-a) \to \infty$, here the number of degrees of freedom needed to maintain accuracy remains bounded as $k(b-a) \to \infty$, as we shall see below.

In figure 4.1 we plot $|\Phi^*|$ and $|\Phi_2|$ for $m = 10$. Noting the logarithmic scales on the plots, it is clear that $|\Phi^*|$ is highly peaked near the discontinuities in impedance. Recalling that Φ is a correction term, namely the difference between the true solution and the solution that there would be if the impedance was constant everywhere, the reason for this is clear. On the plot of $|\Phi_2|$ we also show the two grids Ω_1^+ and Ω_1^-. For s/λ less than about -6 and for s/λ greater than about 6 the grids do not overlap, and on these regions $\Phi_2(s) = e^{\mathrm{i}s}\times$ (piecewise constants) and $\Phi_2(s) = e^{-\mathrm{i}s}\times$ (piecewise constants) respectively. Thus $|\Phi_2(s)|$ is piecewise constant where the grids do not overlap, and this can be clearly seen in figure 4.1. Where the grids overlap, (roughly between $s/\lambda = -6$ and $s/\lambda = 6$) the oscillatory nature of $\Phi_2(s)$ is more apparent.

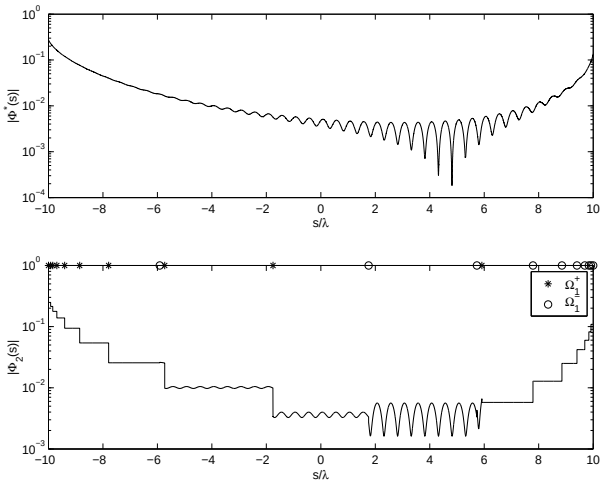

FIG. 4.1. *Plot of* $|\Phi^*|$ *and* $|\Phi_2|$, $m = 10$, *so that* $b - a = 20\lambda$

In figure 4.2 we plot $|\Phi_N|$ for $m = 160$ and for N=2, 4, 8, 16, 32, 64. Again noting the logarithmic scales on each plot, $|\Phi_N|$ is highly peaked near the impedance discontinuities, much more so than for $m = 10$. As N increases so we discretise a larger part of the domain $[-m\lambda, m\lambda]$, as well as having a finer mesh near the discontinuities in impedance at $-m\lambda$, $m\lambda$. For N=2, 4, 8, 16 the piecewise constant approximation can be clearly seen, as the grids Ω_1^+ and Ω_1^- do not overlap. For $N = 32$ the grids overlap between about $s\lambda = -100$ and $s\lambda = 100$. For $N = 64$, each grid covers the whole domain $[-m\lambda, m\lambda]$.

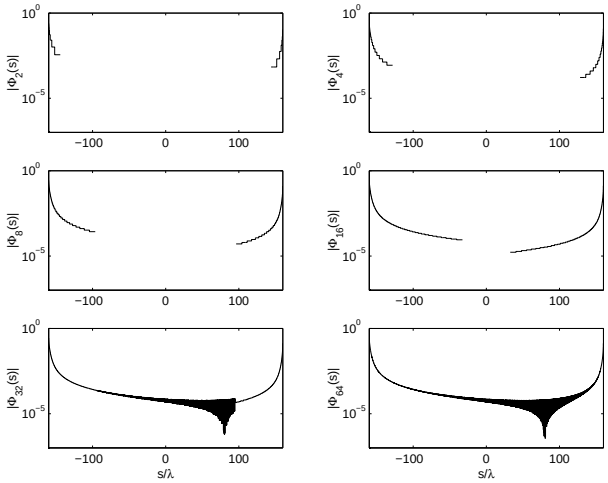

FIG. 4.2. *Plot of* $|\Phi_N|$, $N = 2, 4, 8, 16, 32, 64$ *for* $m = 160$, *so that* $b - a = 320\lambda$

In figure 4.3 we plot $|\Phi^*|$ and $|\Phi^* - \Phi_N|$ for $m = 5120$ and for $N = 4$, 16 and 64. In this case the interval $[-m\lambda, m\lambda]$ is over ten thousand wavelengths long, and so even for $N = 64$ the grids Ω_1^+ and Ω_1^- do not overlap. As m increases, so $|\Phi^*|$ becomes even more peaked, and the benefit of clustering the grid points around the impedance discontinuities becomes even more apparent.

For $m = 10$, 160 and 5120 the relative L_2 errors $\|\Phi^* - \Phi_N\|_2 / \|\Phi^*\|_2$ are shown in Table 4.1. (All L_2 norms are computed by approximating by discrete L_2 norms, sampling at 100000 evenly spaced points in the relevant interval for the function whose norm is to be evaluated.) The estimated order of convergence is given by

$$\text{EOC} := \log_2 \left(\frac{\|\Phi^* - \Phi_N\|_2}{\|\Phi^* - \Phi_{2N}\|_2} \right).$$

For this example, theorem 3.5 predicts that

$$\|\Phi^* - \Phi_N\|_2 \leq \frac{C}{N}(1 + \log^{1/2}(\min(\sqrt{2}\alpha N, 2m\lambda))),$$

so that we expect EOC ≈ 1, and this is what we see. For each value of m, the number of degrees of freedom M_N increases approximately in proportion to $N \log N$ as N increases until the two grids Ω_1^+ and Ω_1^- each cover the whole domain $[-m\lambda, m\lambda]$ (i.e. until $\sqrt{2}\alpha N \geq 2m\lambda$), after which M_N increases only proportionally to N as N increases further. For $m = 10$, the whole domain is covered by the grids for $N = 4$; for $m = 160$ this occurs for $N = 64$ but for $m = 5120$ the two grids do not overlap even

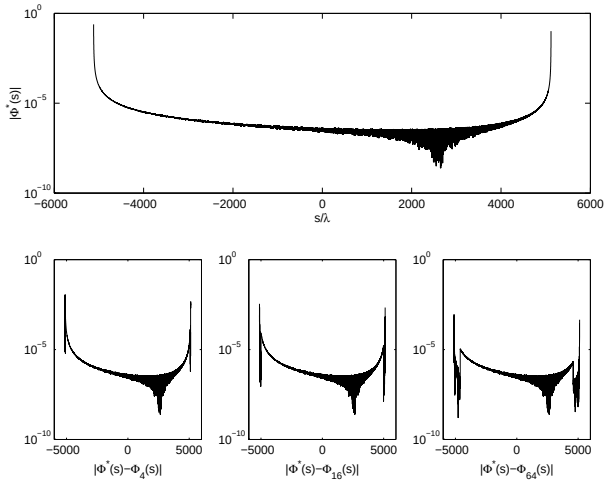

FIG. 4.3. *Plot of* $|\Phi^*|$ *and* $|\Phi^* - \Phi_N|$, $N = 4$, *16, 64 for* $m = 5120$, *so that* $b - a = 10240\lambda$

$(b-a)/\lambda$	N	M_N	$\|\Phi^* - \Phi_N\|_2/\|\Phi^*\|_2$	EOC	COND
20	2	18	1.635×10^{-1}	1.1	1.8
	4	42	7.393×10^{-2}	1.1	2.6
	8	90	3.525×10^{-2}	1.0	8.1
	16	182	1.773×10^{-2}	1.0	94.0
	32	370	8.875×10^{-3}	1.0	625.5
	64	742	4.557×10^{-3}		2551.6
320	2	18	1.647×10^{-1}	1.2	1.8
	4	46	7.399×10^{-2}	1.0	2.0
	8	106	3.622×10^{-2}	1.0	2.0
	16	240	1.790×10^{-2}	1.0	2.1
	32	530	8.662×10^{-3}	0.9	2.1
	64	1094	4.537×10^{-3}		92.7
10240	2	18	1.639×10^{-1}	1.2	1.8
	4	46	6.918×10^{-2}	0.8	2.0
	8	106	3.881×10^{-2}	1.2	2.0
	16	240	1.751×10^{-2}	1.1	2.1
	32	530	8.076×10^{-3}	0.8	2.1
	64	1154	4.579×10^{-3}		2.1

TABLE 4.1
$\|\Phi^* - \Phi_N\|_2/\|\Phi^*\|_2$ *for* $m = 10$, 160 *and* 5120, *and increasing* N.

for $N = 64$. The condition numbers for the matrix of the linear system (4.2) (denoted by COND) satisfy the bound (4.3), which predicts that COND ≤ 3.75, so long as the grids do not overlap, i.e. $N \leq 16$ for $m = 160$, all values of N for $m = 5120$. For $N \leq 32$ the number of degrees of freedom is the same for $m = 160$ and $m = 5120$, and yet the relative L_2 error is almost the same for the two cases $b - a = 320\lambda$ and $b - a = 10240\lambda$.

In Table 4.2 we fix $N = 16$ and show $\|\Phi^* - \Phi_{16}\|_2/\|\Phi^*\|_2$ and also $\|\Phi^* - \Phi_{16}\|_2$ for increasing values of $m = (b - a)/2\lambda$. As m increases, the number of degrees

$(b-a)/\lambda$	M_N	$\|\Phi^* - \Phi_{16}\|_2/\|\Phi^*\|_2$	$\|\Phi^* - \Phi_{16}\|_2$	COND
10	162	1.746×10^{-2}	7.936×10^{-3}	181.5
20	182	1.773×10^{-2}	8.059×10^{-3}	94.0
40	204	1.775×10^{-2}	8.068×10^{-3}	24.7
80	226	1.766×10^{-2}	8.027×10^{-3}	8.2
160	240	1.761×10^{-2}	8.000×10^{-3}	2.1
320	240	1.790×10^{-2}	8.122×10^{-3}	2.1
640	240	1.749×10^{-2}	7.916×10^{-3}	2.1
1280	240	1.650×10^{-2}	7.435×10^{-3}	2.1
2560	240	1.616×10^{-2}	7.216×10^{-3}	2.1
5120	240	1.556×10^{-2}	6.831×10^{-3}	2.1
10240	240	1.751×10^{-2}	7.433×10^{-3}	2.1

TABLE 4.2
$\|\Phi^* - \Phi_{16}\|_2/\|\Phi^*\|_2$ *for increasing interval length.*

of freedom increases logarithmically for those values of m for which $\sqrt{2}\alpha N \geq 2m\lambda$, i.e. for $m \leq 40$, but as m increases further for $m \geq 80$ the number of degrees of freedom remains constant, and yet both the relative and actual L_2 error also remain roughly constant as m grows. For $m = 5120$ the interval is of length greater than ten thousand wavelengths, and yet we achieve almost one per cent relative error with only 240 degrees of freedom. As in table 4.1, the condition number of the linear system (4.2) is bounded by (4.3), so that COND ≤ 3.75, when m is sufficiently large that the grids Ω_1^+ and Ω_1^- do not overlap, i.e. for $m \geq 160$.

In figure 4.4 we plot $|u^t(x)|$ for $x = (x_1, \lambda)$, $x_1 \in [-2m\lambda, 2m\lambda]$, i.e. the absolute value of the total acoustic field one wavelength above the plane, as computed with $\sqrt{2}\alpha = 1000$ and $N = 128$, for $m = 5$ (plot (i)), $m = 10$ (plot (ii)), $m = 20$ (plot (iii)), $m = 40$ (plot (iv)), $m = 80$ (plot (v)) and $m = 160$ (plot (vi)). In each plot the x-axis represents x_1/λ and the y-axis represents $|u^t(x)|$. One can clearly see that the wave diffracted from the impedance discontinuities at $x = (-m\lambda, 0)$ and $x = (m\lambda, 0)$ is a significant component of the total field only within a small number of wavelengths of the impedance discontinuities. Figure 1.1 shows a surface plot of the incident, scattered and total wave fields up to ten wavelengths above the plane for this same example with $m = 5$.

We also computed $u_N^t(x)$ for $x = (m\lambda/2, \lambda)$ and $x = (m\lambda, \lambda)$ for $m = 10$ and $m = 160$ and for $\sqrt{2}\alpha = 50$, $N = 2$, 4, 8, 16, 32 and 64. Taking the values for $\alpha = 500\sqrt{2}$, $N = 128$ to be the "exact" values, the errors are shown in table 4.3. The estimated order of convergence is calculated as

$$\text{EOC} := \log_2 \left(\frac{|u^t(x) - u_N^t|}{|u^t(x) - u_{2N}^t|} \right),$$

and from theorem 3.6 we would expect EOC ≈ 1. The convergence rate is rather irregular, but broadly speaking it is at least as good as expected, and the actual and relative errors are both very small. The value of $|u^t(x)|$ is between 0.7 and 0.9 in each case.

Acknowledgement Some of this work was carried out whilst the authors participated in the 2003 Programme Computational Challenges in Partial Differential Equations at the Isaac Newton Institute, Cambridge, UK.

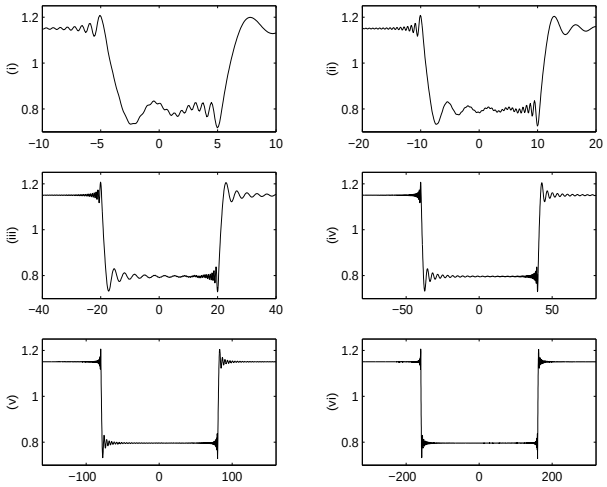

FIG. 4.4. $|u^t(x)|$ *(on the y-axis) against* x_1/λ *(on the x-axis) for* $x = (x_1, \lambda)$, $x_1 \in [-2m\lambda, 2m\lambda]$, *plotted for* $m = 5$ *(plot (i)),* $m = 10$ *(plot (ii)),* $m = 20$ *(plot (iii)),* $m = 40$ *(plot (iv)),* $m = 80$ *(plot (v)) and* $m = 160$ *(plot (vi))*

		$x = (m\lambda/2, \lambda)$		$x = (m\lambda, \lambda)$	
m	N	$\lvert u^t(x) - u_N^t(x)\rvert$	EOC	$\lvert u^t(x) - u_N^t(x)\rvert$	EOC
10	2	3.894×10^{-4}	1.5	1.108×10^{-4}	1.3
	4	1.421×10^{-4}	2.5	4.514×10^{-5}	3.5
	8	2.432×10^{-5}	1.0	4.068×10^{-6}	0.2
	16	1.183×10^{-5}	2.7	3.448×10^{-6}	0.8
	32	1.841×10^{-6}	1.0	2.014×10^{-6}	1.1
	64	9.350×10^{-7}		9.108×10^{-7}	
160	2	1.059×10^{-4}	2.0	5.278×10^{-4}	2.6
	4	2.572×10^{-5}	0.4	8.790×10^{-5}	2.8
	8	1.978×10^{-5}	0.0	1.283×10^{-5}	0.3
	16	1.981×10^{-5}	2.1	1.060×10^{-5}	0.8
	32	4.474×10^{-6}	0.9	6.029×10^{-6}	3.4
	64	2.431×10^{-6}		5.634×10^{-7}	

TABLE 4.3
$|u^t(x) - u_N^t(x)|$ *for* $m = 10$ *and* $m = 160$, *and increasing* N.

REFERENCES

[1] T. ABBOUD, J. NÉDÉLEC, AND B. ZHOU, *Méthodes des équations intégrales pour les hautes fréquences*, C.R. Acad. Sci. I-Math, 318 (1994), pp. 165–170.

[2] M. ABRAMOWITZ AND I. STEGUN, *Handbook of Mathematical Functions*, Dover, 1972.

[3] K. ATKINSON, *The numerical solution of integral equations of the second kind*, Cambridge University Press, 1997.

[4] K. ATTENBOROUGH, *Acoustical impedance models for outdoor ground surfaces*, J. Sound Vib., 99 (1985), pp. 521–544.

[5] I. BABUŠKA AND S. SAUTER, *Is the pollution effect of the FEM avoidable for the Helmholtz equation considering high wave numbers*, SIAM J. Numer. Anal., 34 (1997), pp. 2392–2423. Reprinted in *SIAM Rev.* **42** (3), 451-484, 2000.

[6] P. BOULANGER, K. ATTENBOROUGH, S. TAHERZADEH, T. WATERSFULLER, AND K. LI, *Ground effect over hard rough surfaces*, J Acoust. Soc. Am., 104 (1998), pp. 1474–1482.

[7] O. Bruno and L. Kunyansky, *A fast, high-order algorithm for the solution of surface scattering problems: Basic implementation, tests and applications*, J. Comput. Phys., 169 (2001), pp. 80–110.

[8] O. Cessenat and B. Després, *Application of an ultra weak variational formulation of elliptic PDEs to the two-dimensional Helmholtz problem*, SIAM J. Numer. Anal., 35 (1998), pp. 255–299.

[9] S. Chandler-Wilde, *The impedance boundary value problem for the Helmholtz equation in a half-plane*, Math. Meth. Appl. Sci., 20 (1997), pp. 813–840.

[10] S. Chandler-Wilde and D. Hothersall, *Sound propagation above an inhomogeneous impedance plane*, J. Sound Vib., 98 (1985), pp. 475–491.

[11] ———, *Efficient calculation of the Green's function for acoustic propagation above a homogeneous impedance plane*, J. Sound Vib., 180 (1995), pp. 705–724.

[12] S. Chandler-Wilde, S. Langdon, and L. Ritter, *A high wavenumber boundary element method for an acoustic scattering problem*, Proc. R. Soc. Lond. A, (2003). To appear.

[13] S. Chandler-Wilde, M. Rahman, and C. Ross, *A fast two-grid and finite section method for a class of integral equations on the real line with application to an acoustic scattering problem in the half-plane*, Numer. Math., 93 (2002), pp. 1–51.

[14] S. Christiansen and J. Nedelec, *Preconditioners for the numerical solution of boundary integral equations from electromagnetism*, C.R. Acad. Sci. I-Math, 331 (2000), pp. 733–738.

[15] D. Colton and R. Kress, *Integral Equation Methods in Scattering Theory*, Wiley, 1983.

[16] E. Darrigrand, *Coupling of fast multipole method and microlocal discretization for the 3-D Helmholtz equation*, J. Comput. Phys., 181 (2002), pp. 126–154.

[17] E. Darve, *The fast multipole method: numerical implementation*, J. Comput. Phys., 160 (2000), pp. 195–240.

[18] A. de La Bourdonnaye, *A microlocal discretization method and its utilization for a scattering problem*, C.R. Acad. Sci. I-Math, 318 (1994), pp. 385–388.

[19] P. Gaitan, *Equations Intégrales en Acoustique: Etude des Singularités et Convergence des Algorithmes Numériques*, PhD thesis, Universite de Provence - AIX - Marseille I, 1987.

[20] E. Giladi and J. Keller, *A hybrid numerical asymptotic method for scattering problems*, J. Comput. Phys., 174 (2001), pp. 226–247.

[21] D. Habault, *Sound propagation above an inhomogeneous plane*, J. Sound Vib., 100 (1985), pp. 55–67.

[22] F. Ihlenburg, *Finite Element Analysis of Acoustic Scattering*, Springer-Verlag, New York, 1998.

[23] S. Langdon and S. Chandler-Wilde, *A Galerkin boundary element method for an acoustic scattering problem, with convergence rate independent of frequency. Proc. Fourth U.K. Conf. on Boundary Integral Methods*, Salford University Press, 2003. To appear.

[24] S. Langdon and I. Graham, *Boundary integral methods for singularly perturbed boundary value problems*, IMA J. Numer. Anal., 21 (2001), pp. 217–237.

[25] J. Melenk and I. Babuška, *The partition of unity finite element method: Basic theory and applications*, Comput. Method Appl. M., 139 (1996), pp. 289–314.

[26] P. Monk and D. Wang, *A least squares method for the Helmholtz equation*, Comput. Method Appl. M., 175 (1999), pp. 121–136.

[27] P. Morse and K. Ingard, *Theoretical Acoustics*, McGraw Hill Book Co., New York, 1968.

[28] E. Perrey-Debain, J. Trevelyan, and P. Bettess, *Plane wave interpolation in direct collocation boundary element method for radiation and wave scattering: numerical aspects and applications*, J. Sound Vib., (2003). To appear.

[29] ———, *Use of wave boundary elements for acoustic computations*, J. Comput. Acoust., (2003). To appear.

[30] J. Poirier, A. Bendali, and P. Borderies, *Impedance boundary condition for rapidly oscillating surface scatterers.* In: *Mathematical and Numerical Aspects of Wave Propagation*, Ed. A.Bermudez, D.Gomez, P.Joly and J.E.Roberts, 528-532, SIAM Editors, Philadelphia, 2000.

[31] K. Warnick and W. Chew, *Numerical simulation methods for rough surface scattering*, Wave Random Media, 11 (2001), pp. R1–R30.